Multi-messenger signatures of cosmological magnetic fields

Dmitri Semikoz

APC, Paris

in collaboration with

A.Neronov, Ch.Caprini, A.Korochkin, O.Kalashev, G.Lavaux, A.Roper Pol, M.Ramsoy

2007.14331 2009.14174 2111.10311 2112.08202 2201.05630

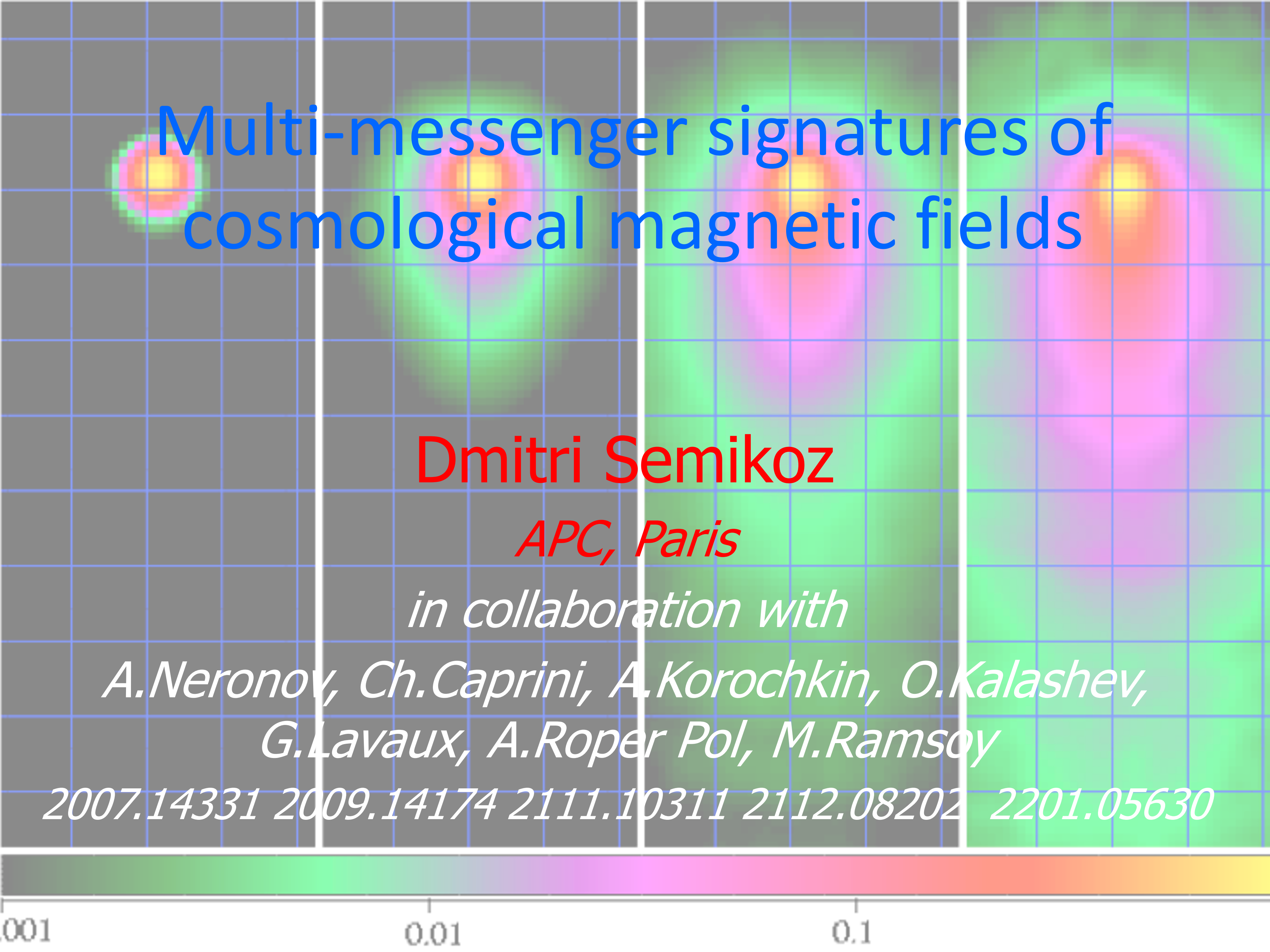

Overview:

- *Introduction: Primordial Magnetic field (PMF) in hot Universe*
- *Pulsar timing arrays: GW from PMF at QCD phase transition*
- *IGMF detection with gamma-rays*
  - *How we can detect cosmologically important IGMF B = 1-10pG*
  - *Detection of IGMF from inflation*
- *IGMF detection with UHECR*
- *Conclusions*

Primordial Magnetic field

Magnetic fields in IGM

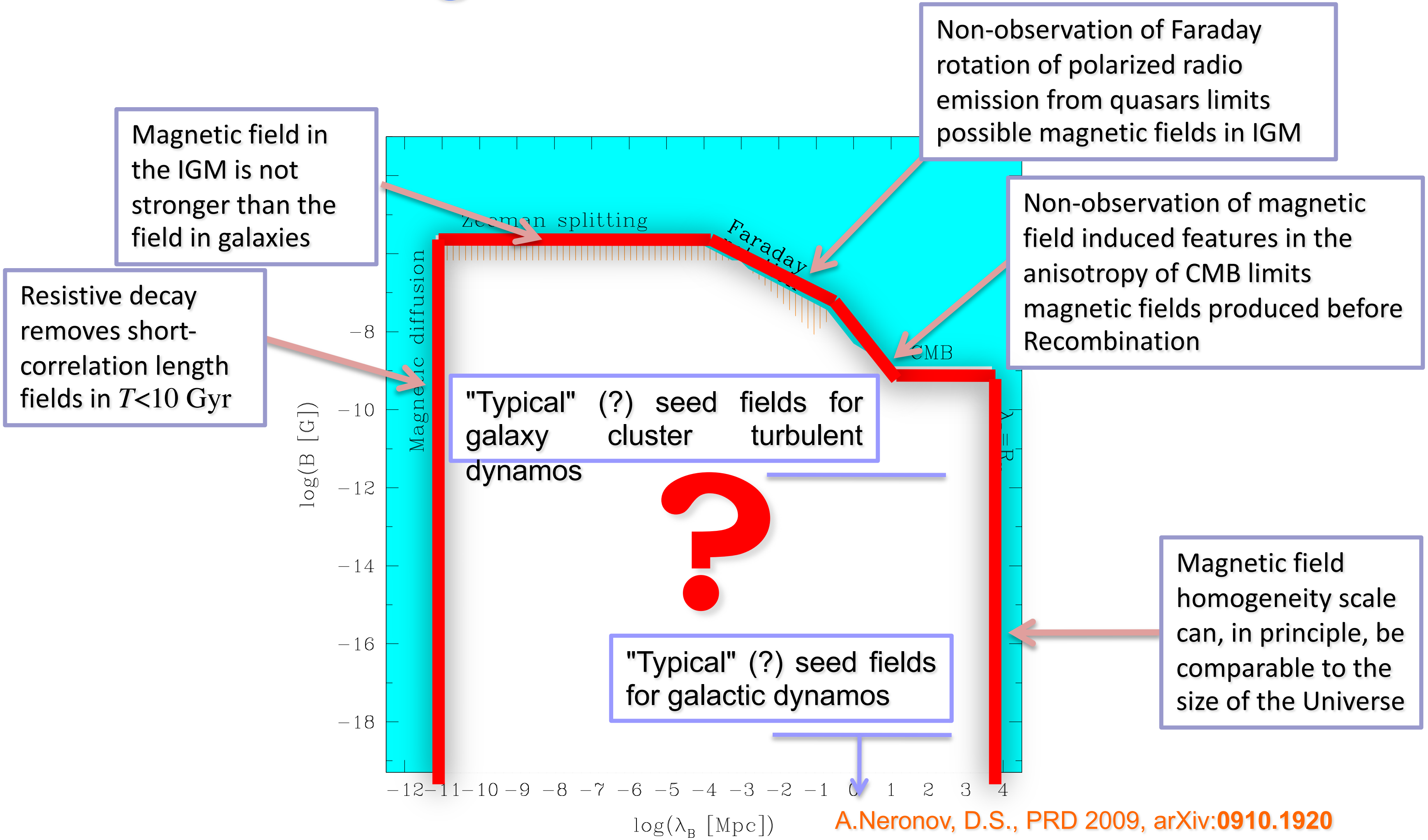

A.Neronov, D.S., PRD 2009, arXiv:**0910.1920**

Produced spectrum of IGMF

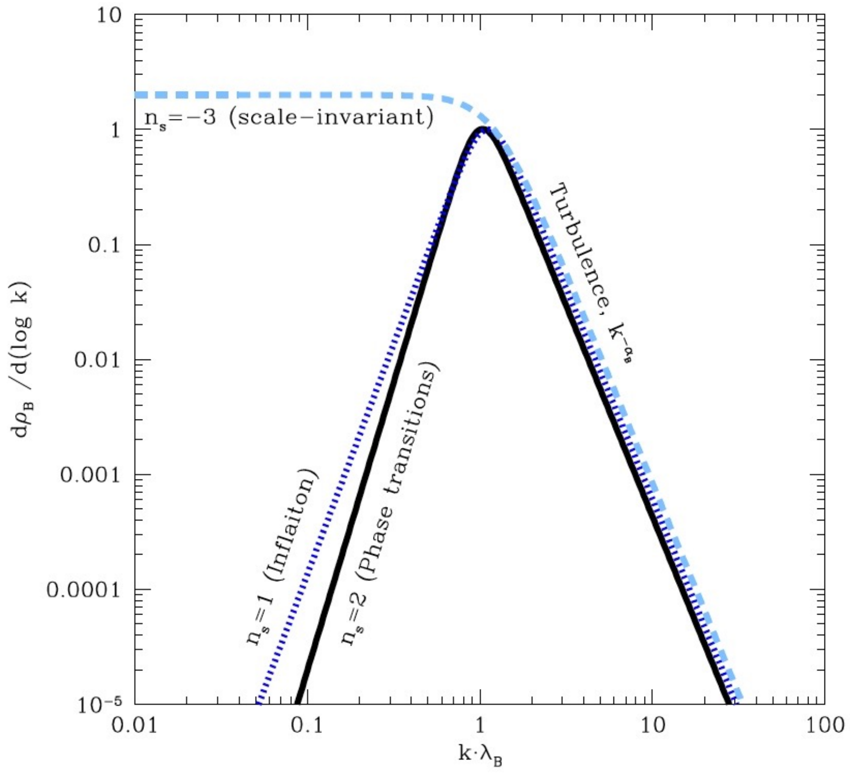

From R.Durrer and A.Neronov, A&A Rev. 21 62, [1303.7121].

Early Universe evolution of spectrum of IGMF

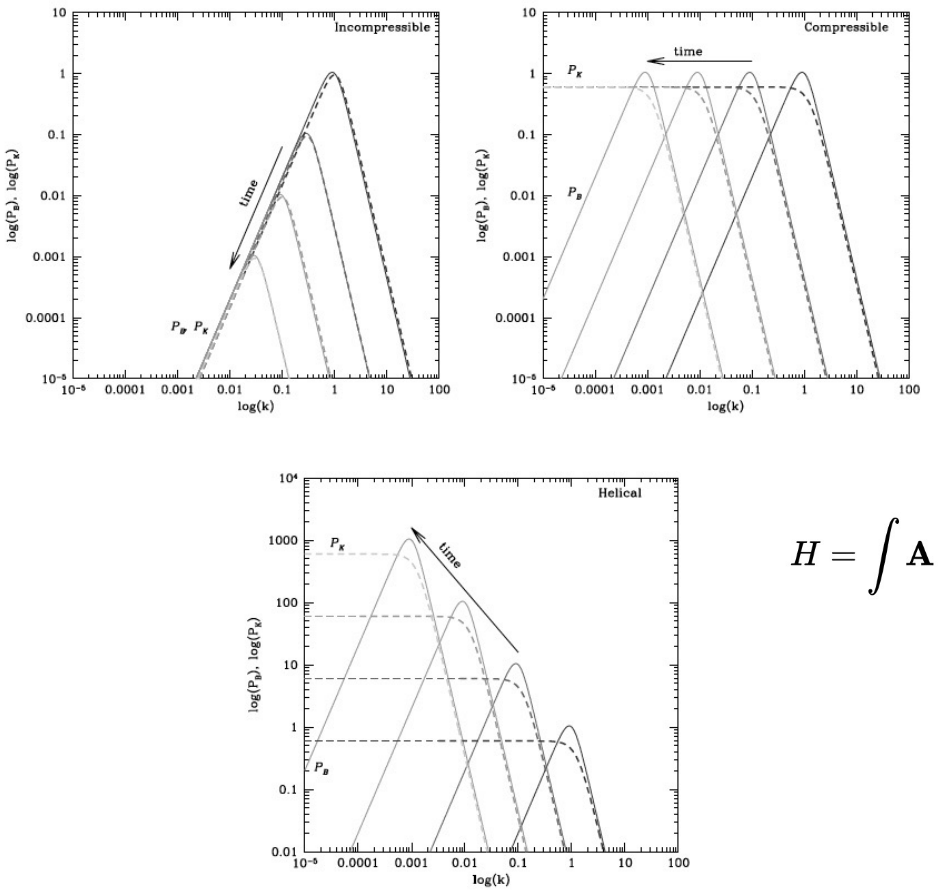

$$H = \int \mathbf{A} \cdot \mathbf{B} \, d^3\mathbf{r}$$

R.Durrer and A.Neronov, A&A Rev. 21 62, [1303.7121].

IGMF from phase transitions

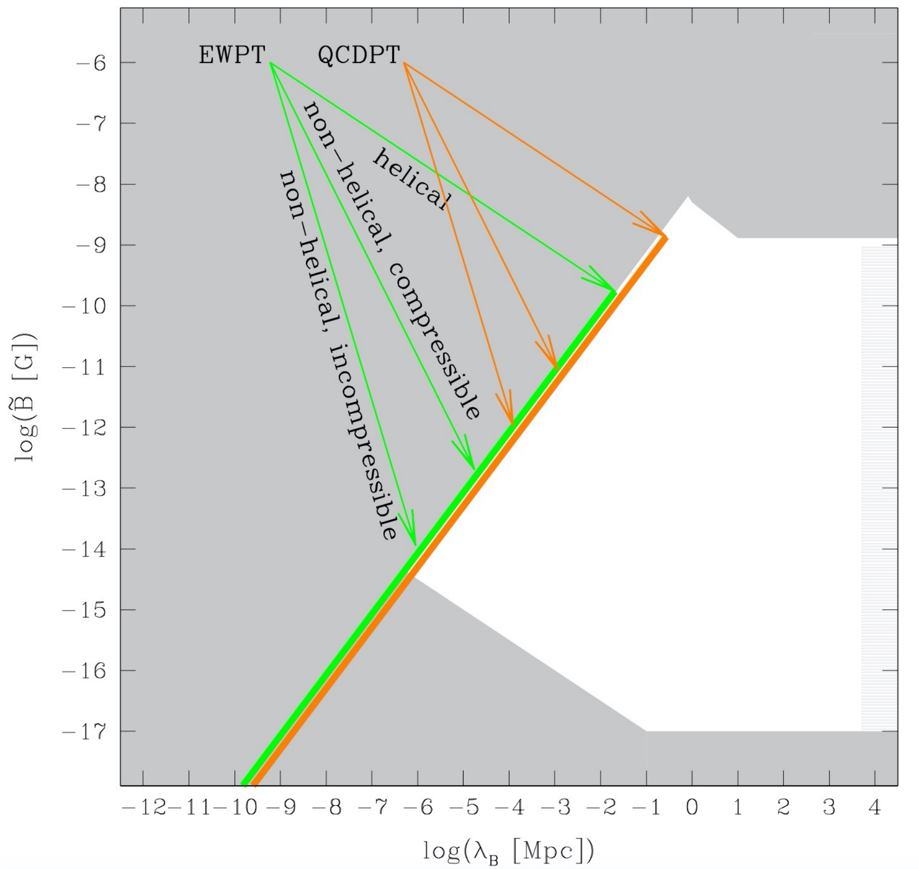

R.Durrer and A.Neronov, A&A Rev. 21 62, [1303.7121].

Detection of IGMF

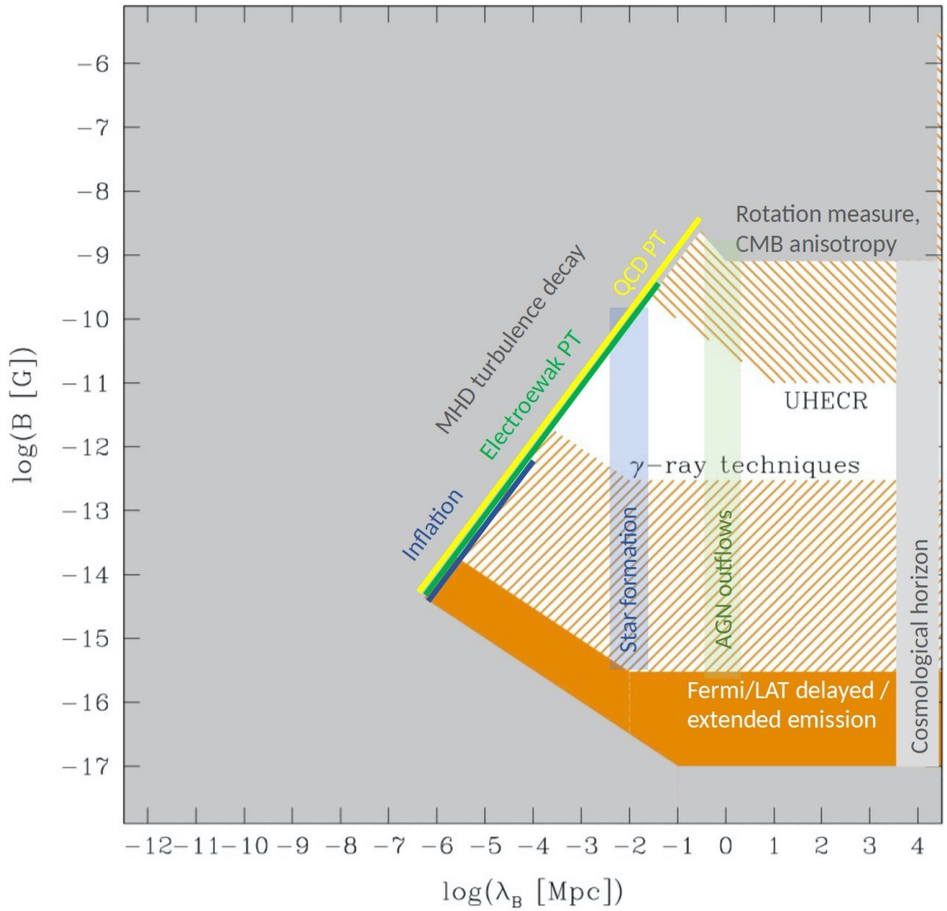

R.Durrer and A.Neronov, A&A Rev. 21 62, [1303.7121].

Constrants on PMF

TABLE I: Constraints on scale-invariant magnetic Fields

Principal effect	Upper limit
Spectral distortions	30 – 40 nG [14–17]
Anisotropic expansion	3.4nG [18]
CMB temp. anisotropies:	
Due to magnetic modes Due to plasma heating	1.2 – 6.4 nG [19–40] 0.63 – 3 nG [16, 38, 41–44]
CMB polarization	1.2nG [21–23, 40, 45–54]
Non-Gaussianity bispectrum	2 – 9 nG [38, 55–64]
Non-Gaussianity trispectrum	0.7nG [65]
Non-Gaussianity trispectrum with inflationary curv. mode	0.05nG [66]
Reionization	0.36 nG [41, 67–70]

H0 with PMF 10-50 pG

	Planck ΛCDM	Planck+H3 ΛCDM	Planck+H3 M1	Planck+H3 M2
$\Omega_b h^2$	0.02237 ± 0.00015	0.02263 ± 0.00014	$0.02270^{+0.00014}_{-0.00016}$	0.02280 ± 0.00016
$\Omega_c h^2$	0.1200 ± 0.0012	0.1172 ± 0.0011	0.1216 ± 0.0014	0.1191 ± 0.0012
τ	0.0546 ± 0.0075	$0.0629^{+0.0075}_{-0.0087}$	0.0555 ± 0.0073	$0.0607^{+0.0071}_{-0.0085}$
n_s	0.9651 ± 0.0041	0.9721 ± 0.0040	0.9628 ± 0.0040	0.9734 ± 0.0042
$b^{(a)}$	-	-	$0.61^{+0.16(0.35)(0.57)}_{-0.20(0.33)(0.42)}$	$0.30 \pm 0.11(0.22)(0.34)$
H_0	67.37 ± 0.54	68.70 ± 0.50	71.03 ± 0.74	69.81 ± 0.62
Ω_m	0.3151 ± 0.0074	0.2977 ± 0.0064	0.2873 ± 0.0064	0.2926 ± 0.0064
σ_8	0.8113 ± 0.0060	0.8080 ± 0.0064	0.8265 ± 0.0079	0.8192 ± 0.0075
S_8	0.831 ± 0.013	0.805 ± 0.012	0.809 ± 0.012	0.809 ± 0.012
z_*	1089.91 ± 0.26	1089.35 ± 0.24	$1107.9^{+4.2}_{-3.6}$	$1096.8^{+2.6}_{-2.0}$
r_*	144.44 ± 0.27	144.96 ± 0.25	142.22 ± 0.65	143.69 ± 0.48
$z_{\rm drag}$	1059.94 ± 0.30	1060.33 ± 0.29	$1076.9^{+3.8}_{-3.4}$	$1067.4^{+2.4}_{-2.0}$
$r_{\rm drag}$	147.10 ± 0.27	147.55 ± 0.25	144.89 ± 0.64	146.28 ± 0.49
$r_{\rm drag} h$	99.11 ± 0.93	101.36 ± 0.87	102.91 ± 0.92	102.11 ± 0.89
$\chi^2_{\rm lensing}$	9.23 ± 0.70 (8.73)	9.6 ± 1.2 (8.74)	9.20 ± 0.66 (8.91)	9.33 ± 0.80 (9.39)
$\chi^2_{\rm plik}$	2359.5 ± 6.2 (2347.6)	2364.0 ± 6.6 (2350.93)	2366.2 ± 6.7 (2355.6)	2367.4 ± 7.1 (2359.2)
$\chi^2_{\rm lowl}$	23.40 ± 0.86 (23.18)	22.36 ± 0.72 (22.76)	24.30 ± 0.97 (24.0)	22.37 ± 0.72 (21.9)
$\chi^2_{\rm simall}$	397.0 ± 1.8 (396.0)	399.0 ± 3.3 (397.2)	397.0 ± 1.7 (395.6)	398.2 ± 2.7 (396.3)
$\chi^2_{\rm prior}$	11.6 ± 4.6 (4.46)	11.6 ± 4.6 (4.38)	11.6 ± 4.5 (4.21)	11.9 ± 4.6 (3.42)
$\chi^2_{\rm CMB}$	2789.1 ± 6.4 (2775.5)	2794.9 ± 7.2 (2779.7)	2796.8 ± 6.9 (2784.2)	2797.3 ± 7.3 (2786.8)
$\chi^2_{\rm H3}$	-	22 ± 4 (24.92)	6.1 ± 3.4 (5.74)	12.9 ± 4.2 (9.62)
$\chi^{2({\rm tot})}_{\rm bestfit}$	2779.9	2809.0	2794.1	2799.9

K.Jedamzik and L. Pogosian 2004.09487

IGMF from QCD phase transition

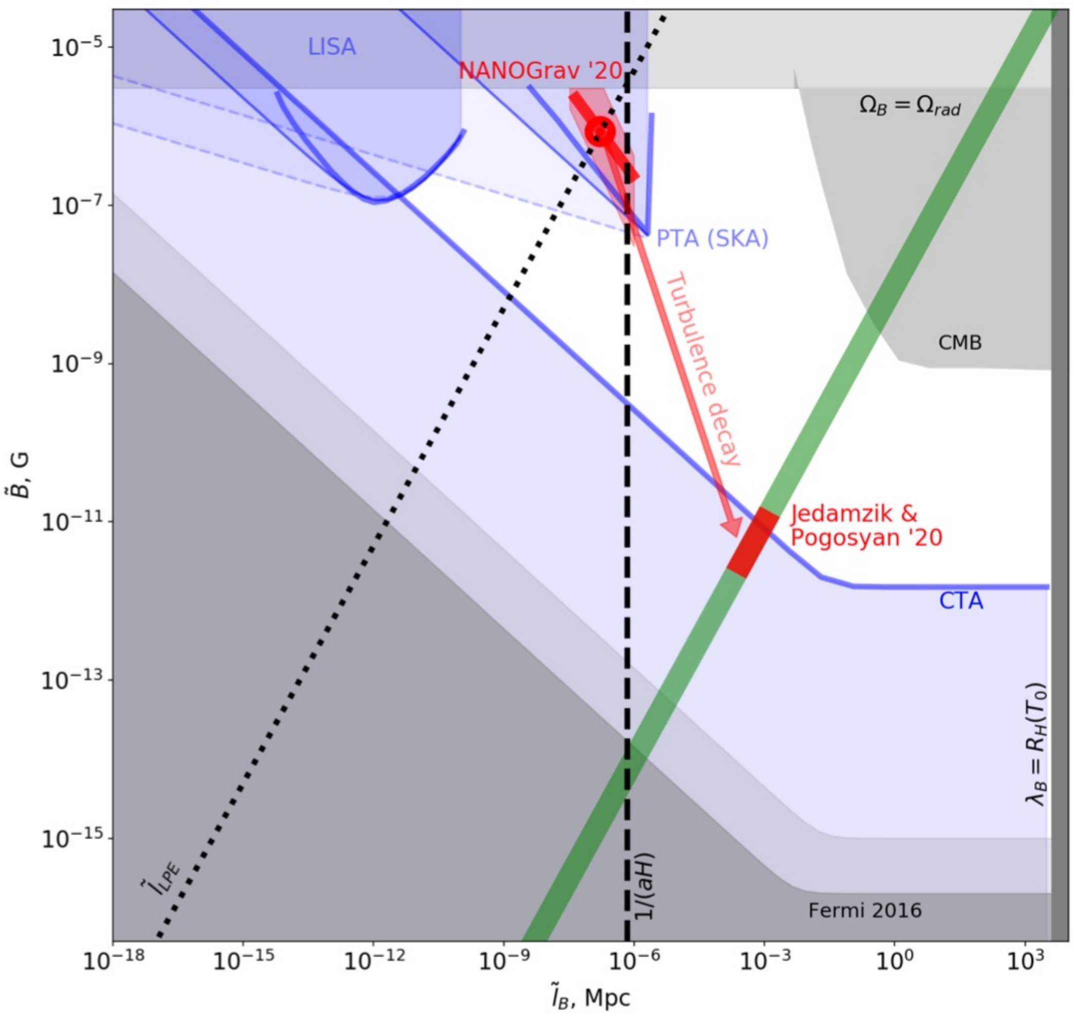

A. Neronov et al., 2009.14174

Pulsar Timing Arrays

Idea: use pulsars as clocks

1978SvA....22...36S

Opportunities for detecting ultralong gravitational waves

M. V. Sazhin

Shternberg Astronomical Institute, Moscow

(Submitted June 14, 1977)

Astron. Zh. **55**, 65–68 (January–February 1978)

The influence of ultralong gravitational waves on the propagation of electromagnetic pulses is examined. Conditions are set forth whereby it might be possible to detect gravitational waves arriving from binary stars. There are some prospects for detecting gravitational radiation from double superstars with masses $\mathfrak{M}_1 \approx \mathfrak{M}_2 \approx 10^{10}\,\mathfrak{M}_\odot$.

PACS numbers: 97.80.–d, 97.60.Gb, 95.30.Gv

The Parkes Pulsar Timing Array Project

Collaborators:

- Australia Telescope National Facility, CSIRO

  Dick Manchester, George Hobbs, Russell Edwards, John Sarkissian, John Reynolds, Mike Kesteven, Grant Hampson, Andrew Brown
- Swinburne University of Technology

  Matthew Bailes, Ramesh Bhat, Joris Verbiest, Albert Teoh
- University of Texas, Brownsville

  Rick Jenet, Willem van Straten
- University of Sydney

  Steve Ord
- National Observatories of China, Beijing

  Xiaopeng You
- Peking University, Beijing

  Kejia Lee
- University of Tasmania

  Aidan Hotan

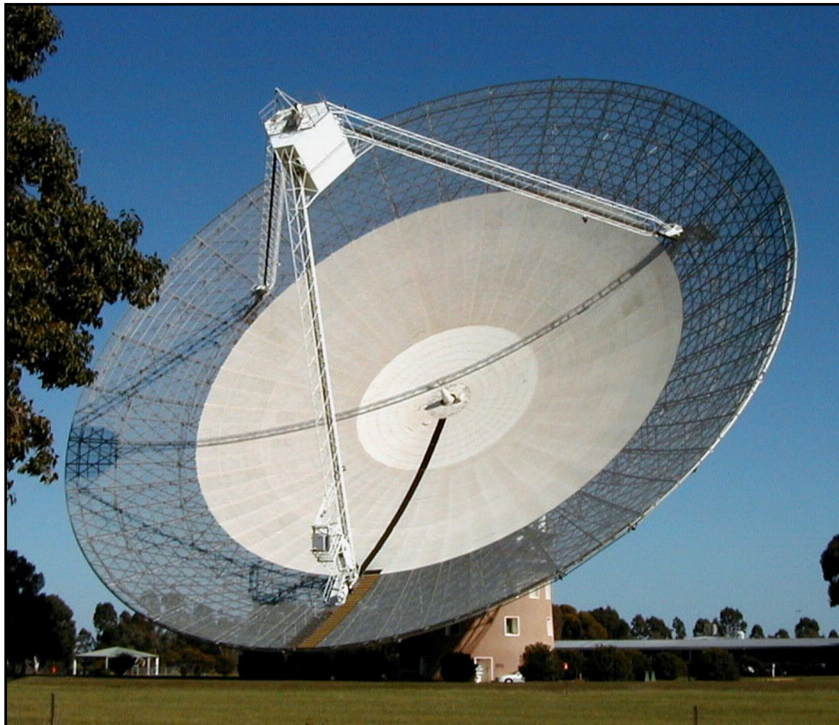

The Gravitational Wave Spectrum

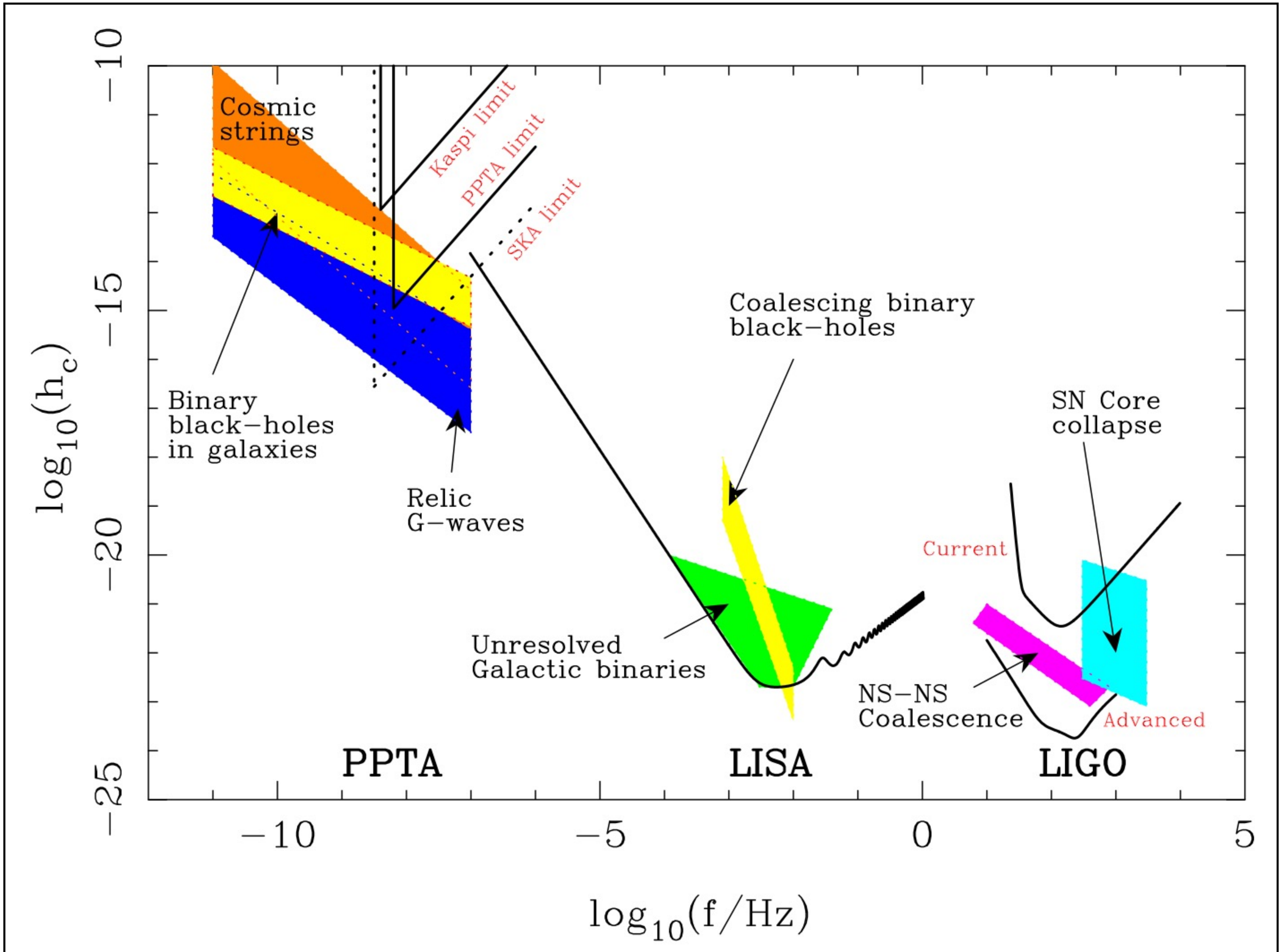

NANOGrav

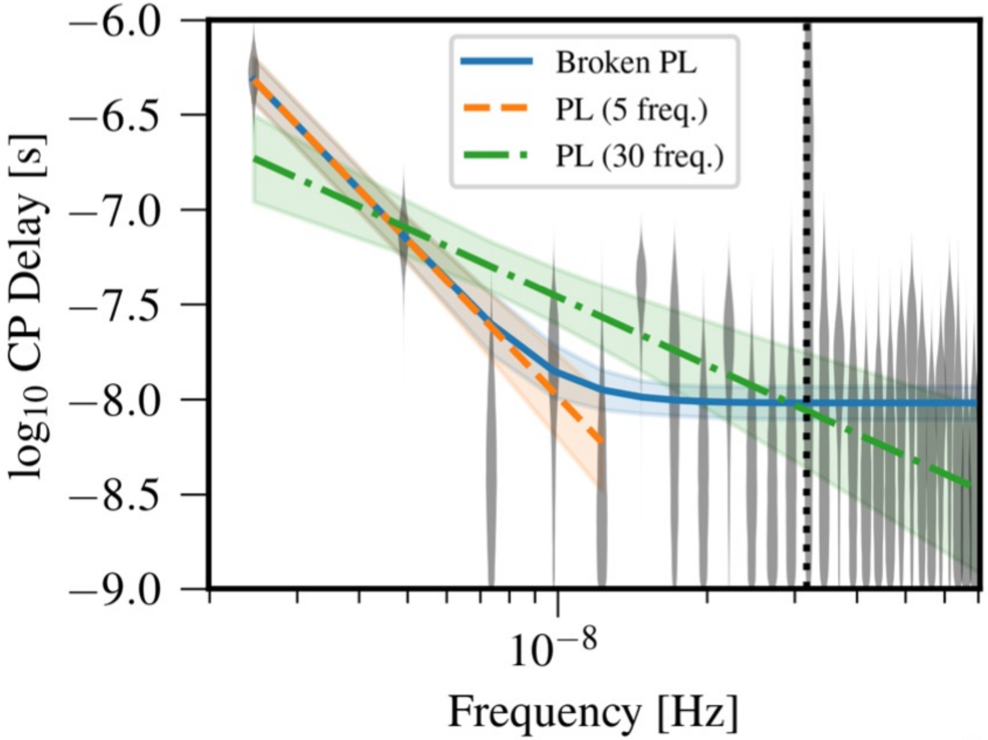

$$S(f) = \frac{A_{\rm CP}^2}{12\pi^2}\left(\frac{f}{f_{\rm yr}}\right)^{-\gamma} f_{\rm yr}^{-3},$$

$$S(f) = \frac{A_{\rm CP}^2}{12\pi^2}\left(\frac{f}{f_{\rm yr}}\right)^{-\gamma}\left(1+\left(\frac{f}{f_{\rm bend}}\right)^{1/\kappa}\right)^{\kappa(\gamma-\delta)} f_{\rm yr}^{-3},$$

NANOGrav Collaboration, 2009.04496

NANOGrav

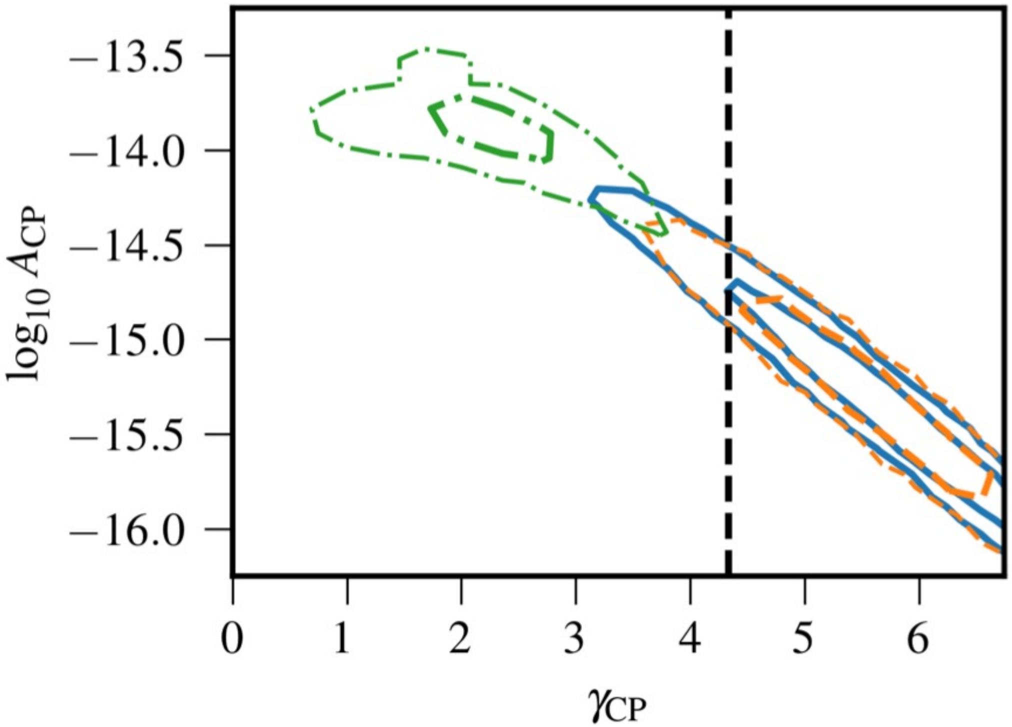

NANOGrav Collaboration, 2009.04496

NANOGrav

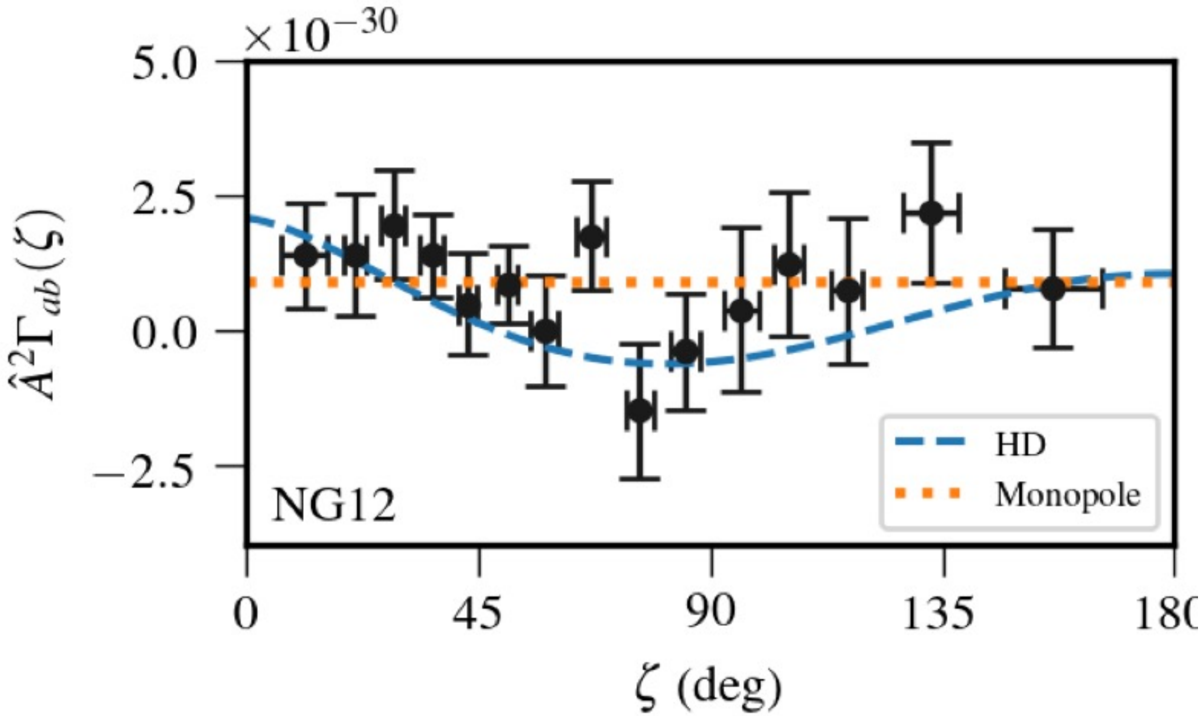

NANOGrav Collaboration, 2009.04496

GW from Primordial Magnetic Field at QCD phase transition

MHD in hot universe

$$\mathrm{d}s^2 = a^2(t)\left[-\mathrm{d}t^2 + \delta_{ij}\,\mathrm{d}x^i\,\mathrm{d}x^j\right], \tag{1}$$

are [3, 6, 54]

$$\begin{aligned}
\frac{\partial \ln \rho}{\partial t} &= -\frac{4}{3}\left(\boldsymbol{\nabla}\cdot\boldsymbol{u} + \boldsymbol{u}\cdot\ln\rho\right) \\
&\quad + \frac{1}{\rho}\left[\boldsymbol{u}\cdot(\boldsymbol{J}\times\boldsymbol{B}) + \eta\boldsymbol{J}^2\right], && (2)\\
\frac{\partial \boldsymbol{u}}{\partial t} &= -\boldsymbol{u}\cdot\boldsymbol{\nabla}\boldsymbol{u} + \frac{\boldsymbol{u}}{3}\left(\boldsymbol{\nabla}\cdot\boldsymbol{u} + \boldsymbol{u}\cdot\boldsymbol{\nabla}\ln\rho\right) \\
&\quad - \frac{\boldsymbol{u}}{\rho}\left[\boldsymbol{u}\cdot(\boldsymbol{J}\times\boldsymbol{B}) + \eta\boldsymbol{J}^2\right] - \frac{1}{4}\boldsymbol{\nabla}\ln\rho \\
&\quad + \frac{3}{4\rho}\boldsymbol{J}\times\boldsymbol{B} + \frac{2}{\rho}\boldsymbol{\nabla}\cdot(\rho\nu\boldsymbol{S}), && (3)\\
\frac{\partial \boldsymbol{B}}{\partial t} &= \boldsymbol{\nabla}\times(\boldsymbol{u}\times\boldsymbol{B} - \eta\boldsymbol{J}), \quad \boldsymbol{J} = \boldsymbol{\nabla}\times\boldsymbol{B}, && (4)
\end{aligned}$$

where ρ is the energy density, $\boldsymbol{J}$ the current density, $S_{ij} = \frac{1}{2}(u_{i,j} + u_{j,i}) - \frac{1}{3}\boldsymbol{\nabla}\cdot\boldsymbol{u}$ the rate-of-strain tensor, ν the kinematic viscosity, and η the magnetic diffusivity. The space coordinates are comoving with

A. Roper Pol et al., 2201.05630

MHD in hot universe

The (normalised) magnetic stress tensor components are $T_{ij}(\boldsymbol{x},t) = -B_i(\boldsymbol{x},t)B_j(\boldsymbol{x},t) + \frac{1}{2}\delta_{ij}\boldsymbol{B}^2(\boldsymbol{x},t)$, and the traceless and transverse (TT) projection of the stress tensor in Fourier space is $\tilde{\Pi}_{ij}(\boldsymbol{k},t) = \tilde{T}_{ij}^{\mathrm{TT}}(\boldsymbol{k},t) = \Lambda_{ijlm}(\hat{\boldsymbol{k}})\tilde{T}_{lm}(\boldsymbol{k},t)$, with $\Lambda_{ijlm} = P_{il}P_{jm} - \frac{1}{2}P_{ij}P_{lm}$. The TT-projected stress Π_{ij} sources the GWs. As $B_i(\boldsymbol{x},t)$, Π_{ij} is also a ran-

$$\langle \Pi_{ij}(\boldsymbol{x},t_1)\,\Pi_{ij}(\boldsymbol{x},t_2)\rangle = \int_0^\infty E_\Pi(k,t_1,t_2)\,\mathrm{d}k.$$

$$\begin{aligned} E_\Pi(k,t_1,t_2) = \frac{k^2}{4\pi}\int \frac{\mathrm{d}^3\boldsymbol{p}}{p^2|\boldsymbol{k}-\boldsymbol{p}|^2} E_\mathrm{M}(p,t_1,t_2) \\ \times E_\mathrm{M}(|\boldsymbol{k}-\boldsymbol{p}|,t_1,t_2)\left(1+(\hat{\boldsymbol{k}}\cdot\hat{\boldsymbol{p}})^2\right) \\ \times \left(1+(\hat{\boldsymbol{k}}\cdot\widehat{\boldsymbol{k}-\boldsymbol{p}})^2\right). \end{aligned} \tag{11}$$

A. Roper Pol et al., 2201.05630

GW production by PMF

GWs are defined as the metric tensor perturbations $\bar{h}_{ij}$ over the FLRW metric, defined in Eq. (1),

$$\mathrm{d}s^2 = a^2(t)\,\left[-\,\mathrm{d}t^2 + (\delta_{ij} + \bar{h}_{ij})\,\mathrm{d}x^i\,\mathrm{d}x^j\right]. \quad (12)$$

$$\left(\partial_t^2 + \boldsymbol{k}^2\right)\tilde{h}_{ij}(\boldsymbol{k},t) = \frac{6\,\tilde{\Pi}_{ij}(\boldsymbol{k},t)}{t}, \quad (13)$$

$$\tilde{h}_{ij}(\boldsymbol{k},t) = \frac{6}{k}\int_{t_*}^{t_{\mathrm{fin}}} \frac{\tilde{\Pi}_{ij}(\boldsymbol{k},t_1)}{t_1}\sin k(t-t_1)\,\mathrm{d}t_1. \quad (14)$$

$$\begin{aligned}\Omega_{\mathrm{GW}}(t) &= \tfrac{1}{12}\left\langle\left(\partial_t h_{ij}(\mathbf{x},t) - h_{ij}(\mathbf{x},t)/t\right)^2\right\rangle \\ &= \int_{-\infty}^{\infty}\Omega_{\mathrm{GW}}(k,t)\,\mathrm{d}\ln k, \quad (15)\end{aligned}$$

A. Roper Pol et al., 2201.05630

Pulsar timing arrays

$$S(f) = \frac{A_{\rm CP}^2}{12\pi^2}\left(\frac{f}{f_{\rm yr}}\right)^{-\gamma} f_{\rm yr}^{-3},$$

$$h_{\rm c}(f) = \sqrt{12\pi^2 S(f) f^3} = A_{\rm CP}\left(\frac{f}{f_{\rm yr}}\right)^{\frac{3-\gamma}{2}}$$

$$\Omega_{\rm GW}^0(f) = \Omega_{\rm yr}\left(\frac{f}{f_{\rm yr}}\right)^{\beta},$$

$$\Omega_{\rm yr} = \frac{2\pi^2}{3H_0^2} f_{\rm yr}^2 A_{\rm CP}^2, \quad \beta = 5-\gamma.$$

A. Roper Pol et al., 2201.05630

Pulsar timing arrays

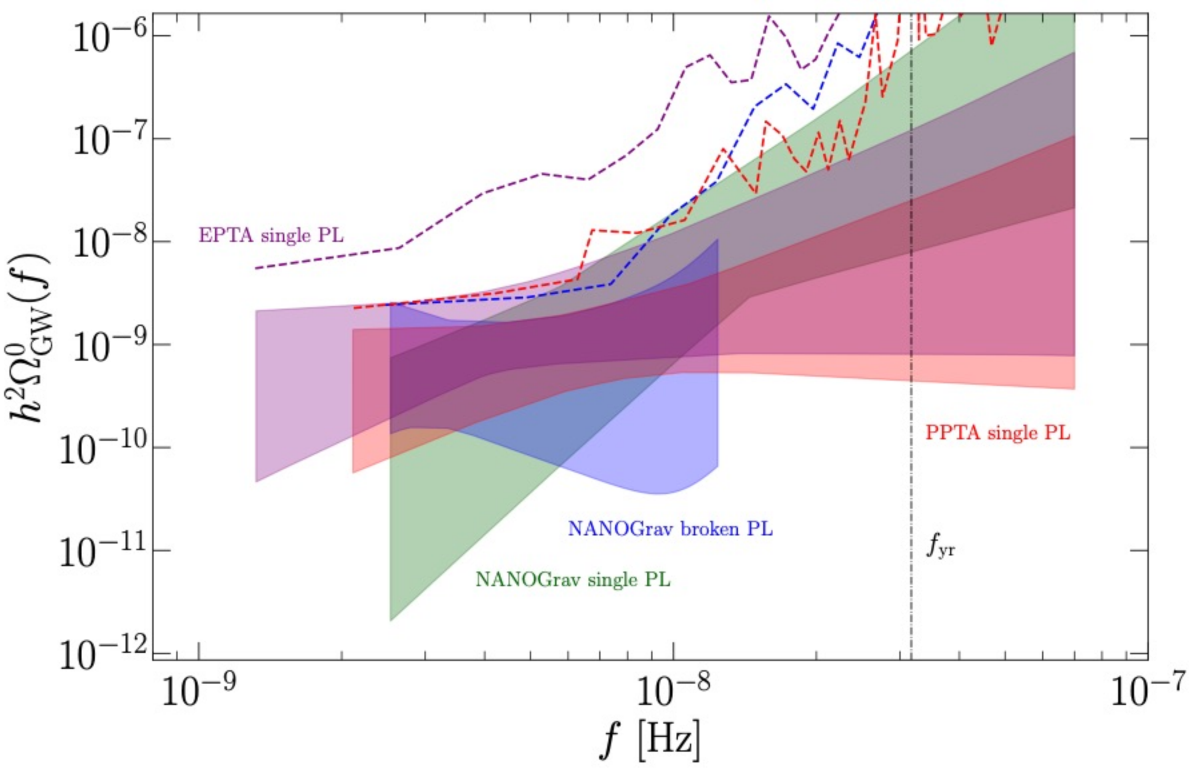

A. Roper Pol et al., 2201.05630

Pulsar timing arrays

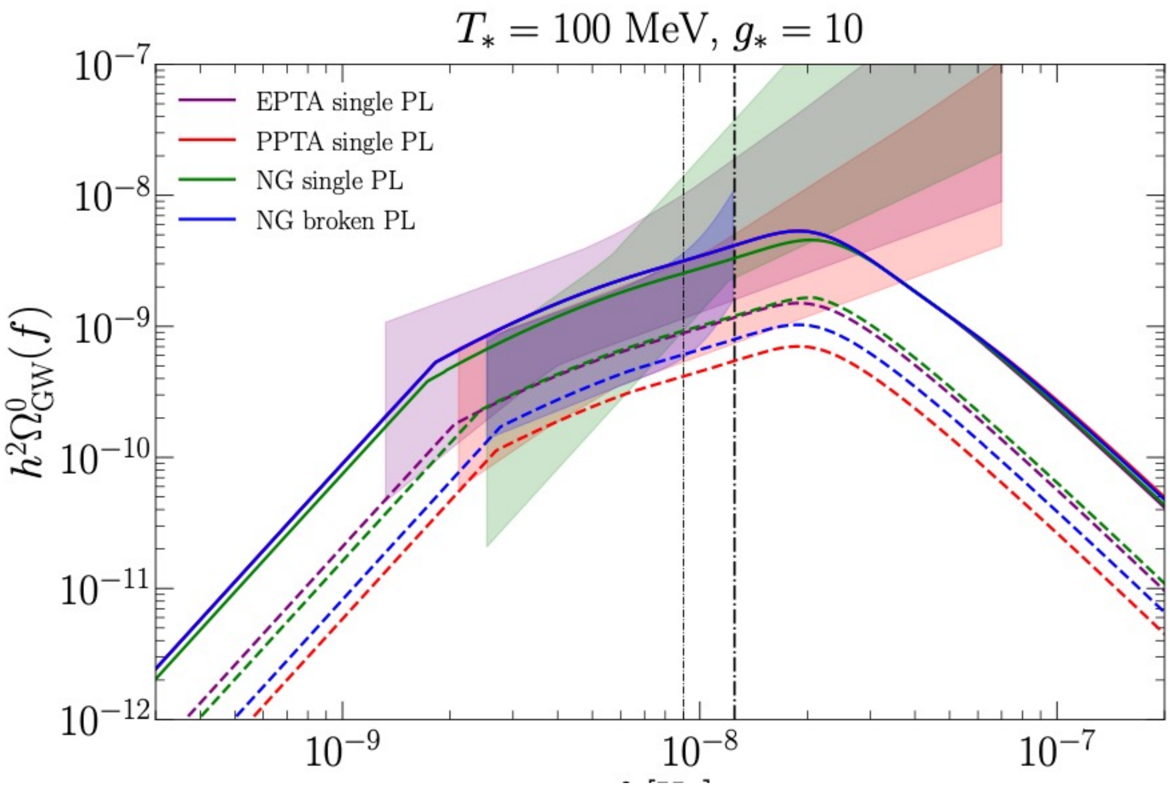

A. Roper Pol et al., 2201.05630

Primordiam magnetic field and SGWB

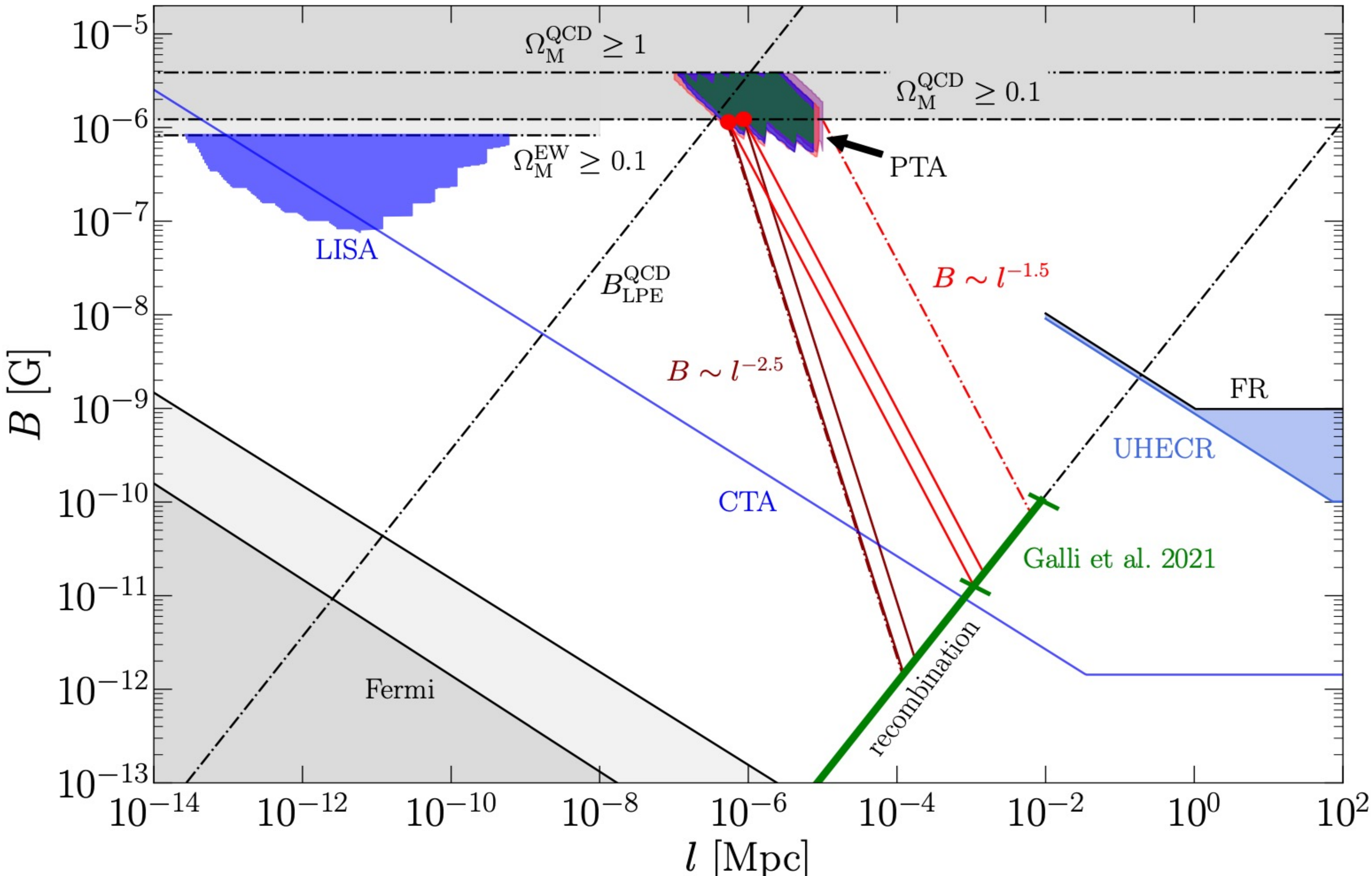

SGWB from SMBH binaries

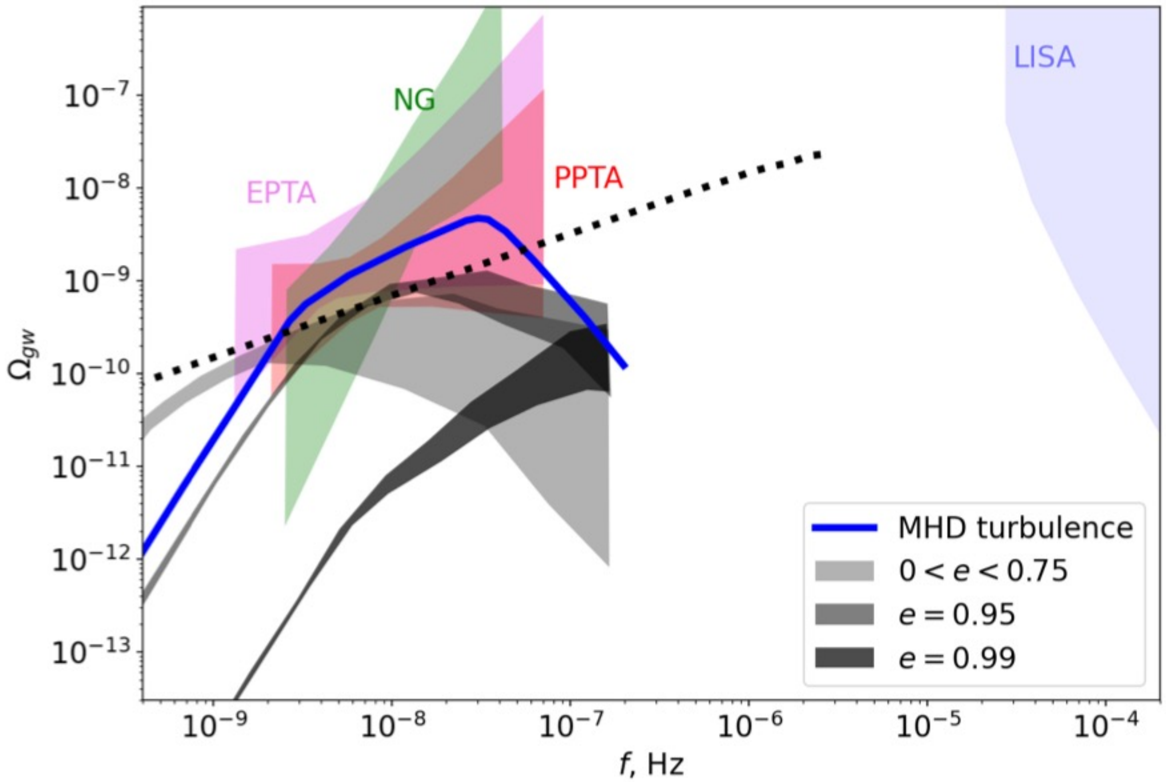

A. Roper Pol et al., 2201.05630

Inter-Galactic Magnetic Field detection with gamma-rays

IGMF measurement with gamma-ray telescopes

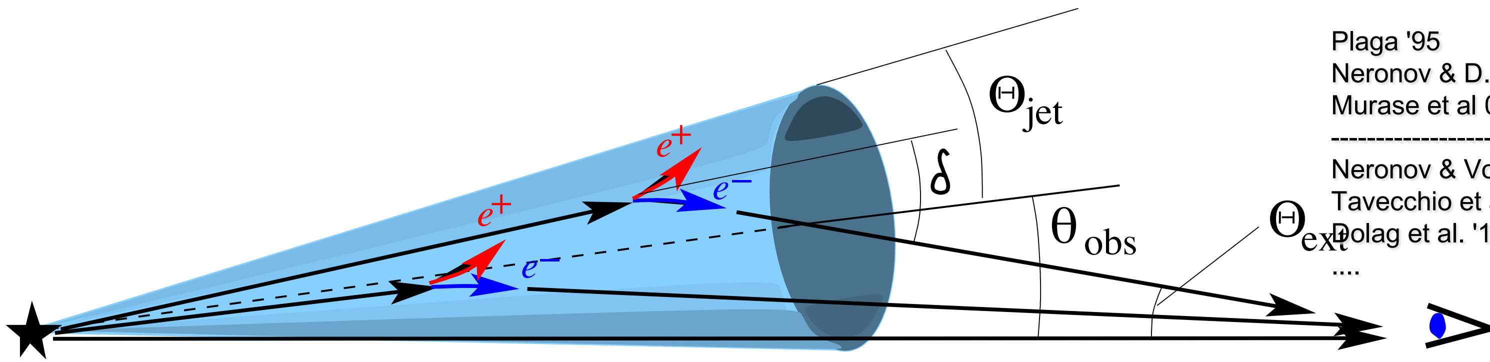

Plaga '95
Neronov & D.S. '07, '09
Murase et al 08

Neronov & Vovk '10
Tavecchio et al. '10
Dolag et al. '10
....

γ-rays with energies above ~0.1 TeV are absorbed by the pair production on the way from the source to the Earth.

$$D_{\gamma_0} = \frac{1}{n_{\rm IR}\sigma_{PP}} \propto 150 \text{ Mpc} \frac{4 \text{ TeV}}{\text{E}} \frac{10 nW/(m^2 sr)}{(\nu F(\nu))_{IR}}$$

$$E_{\gamma 0} = 2E_e \qquad \lambda_e = \frac{1}{n_{\rm CMB}\sigma_{ICS}} \sim 1 \text{ kpc}$$

e^+e^- pairs re-emit γ-rays via inverse Compton scattering of CMB photons.

$$E_\gamma = 12 \text{ GeV} \left(\frac{E_e}{2\text{TeV}}\right)^2$$

Inverse Compton γ-rays could be detected at lower energies.

Cascade component

- Fraction of electron energy in secondary photons in direction of observer

$$\alpha = \frac{\sum E_\gamma}{E_e}$$

- Fraction of voids on the way of primary photon

$$D_{void} = \Delta D_{\gamma_0}$$

- Ratio of point source flux at E_γ and $E_{\gamma 0}$

$$R = F(E_{\gamma_0}) / F(E_\gamma)$$

$$\mathrm{F_{ext}} = \alpha \cdot \mathrm{R} \cdot \Delta \cdot \mathrm{e}^{-\tau(\mathrm{E}_\gamma, \mathrm{z})} \left\langle F_{PS}(E_\gamma) \right\rangle$$

• Search for the GeV cascade signal in Fermi data

Neronov, Vovk '10

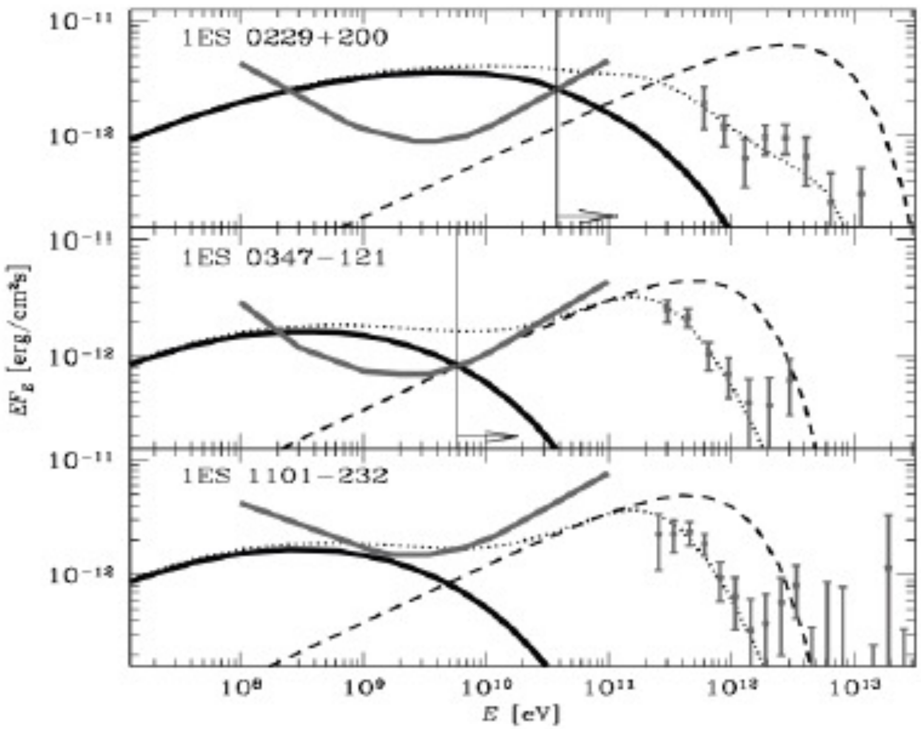

•Search for the GeV counterparts of the hard spectrum far-away sources of TeV gamma-rays within 1 year of Fermi telescope exposure did not reveal the cascade emission component.

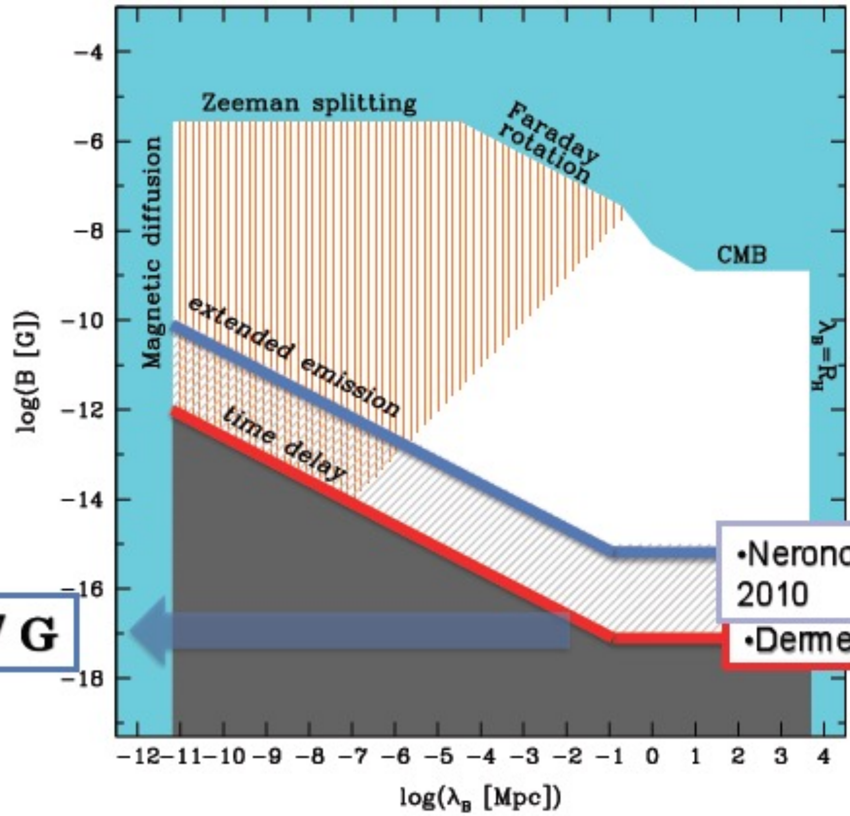

•Neronov, Vovk, 2010, Tavecchio et al. 2010

•Dermer et al., 2011, Taylor et al. 2011

•$B_{\rm IGM} > 10^{-17}$ G

•Non-detection of the cascade signal in the GeV band indicates that electrons and positrons are deflected by non-negligible IGMF which should have strength in excess of 10^{-17} G.

The hardest VHE blazar 1ES 0229+200

Blazar 1ES 0229+200 is considered to be the best candidate for the search of the cascade emission because it has very hard VHE spectrum extending into the ~10 TeV energy band, where γ-ray emission is strongly attenuated by the pair production effect.

Most of the primary γ-ray beam power is removed and transferred to the cascade emission which should appear in the GeV energy band.

The source is extremely weak in the Fermi energy band. It is detected only in the 3-year long exposure.

The source is stable in the VHE band: no variability is found between observations made over ~5 yr time span.

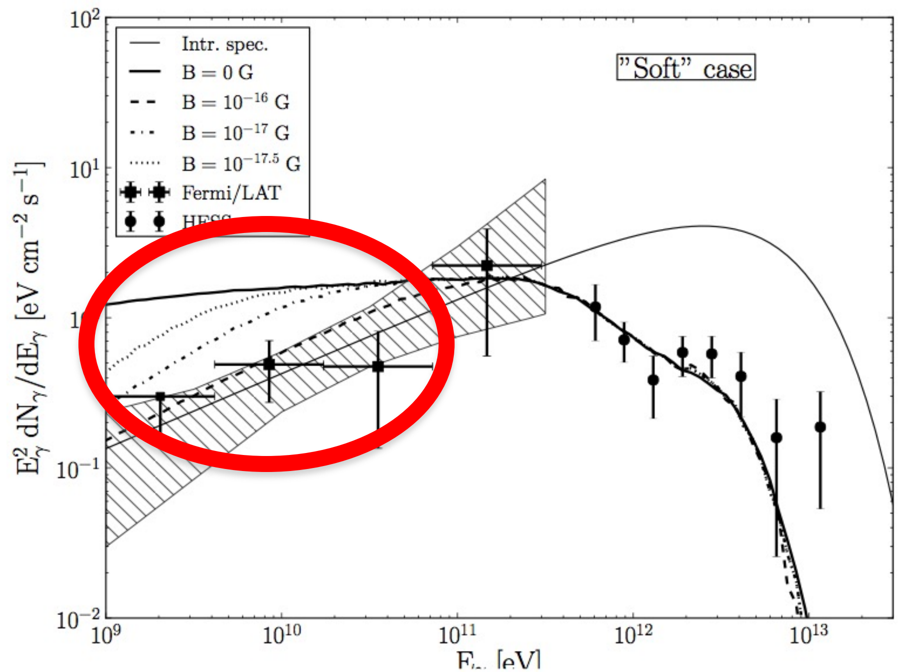

$$\Gamma = 1.36 \pm 0.25$$

Vovk, Taylor, Neronov, and DS 1112.2534

Constraints on IGMF

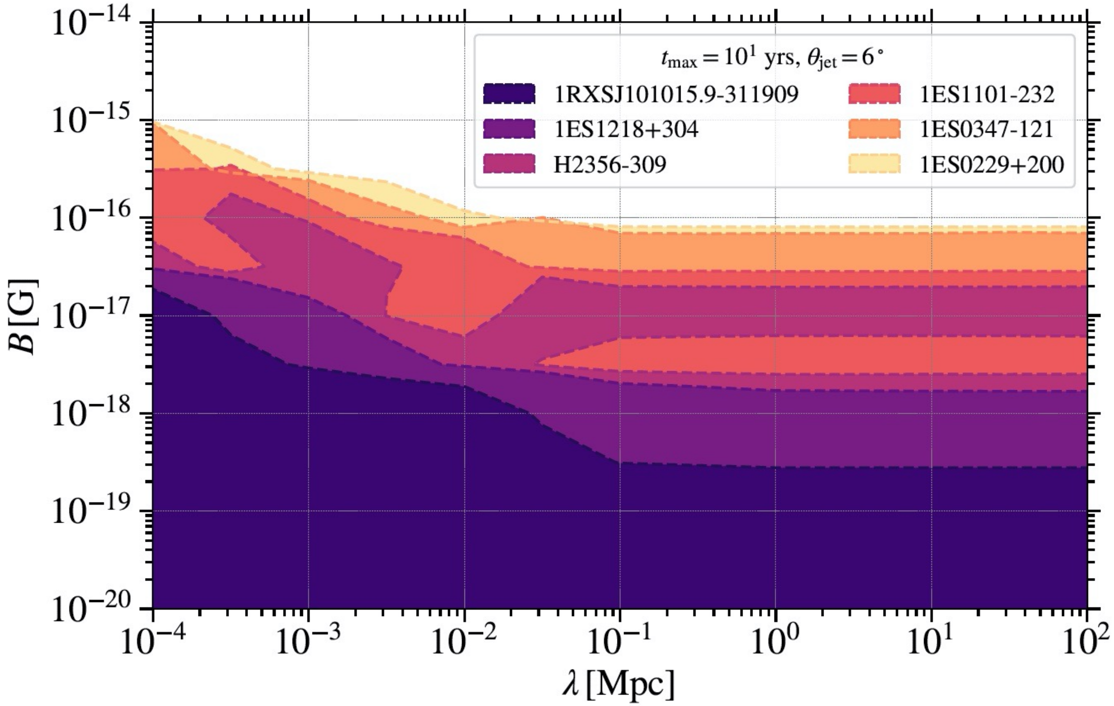

J.Biteau et al, Fermi-LAT ApJS 237 (Aug, 2018) 32, [1804.08035].

Can gamma-telescopes detect 10 pG IGMF (one which can help with H0 problem)?

Detection of IGMF

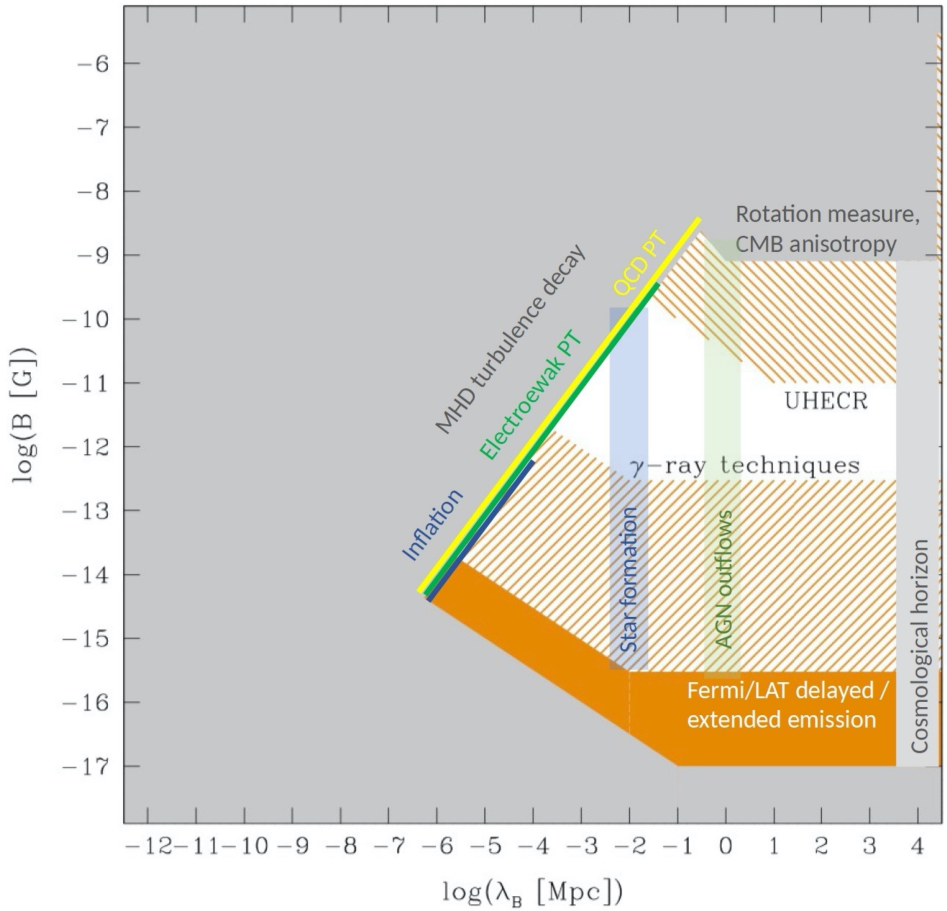

R.Durrer and A.Neronov, A&A Rev. 21 62, [1303.7121].

Detection of 10 pG IGMF

Cosmological IGMF

$$B \sim 10^{-11} \left[\frac{\lambda_B}{1 \text{ kpc}}\right] \text{ G}$$

Primary photon optical depth distance

$$\lambda_{\gamma 0} \simeq 2.5 \left[\frac{E_{\gamma 0}}{100 \text{ TeV}}\right]^{-1.6} \text{ Mpc}$$

Electron travel energy loss distance

$$D_e \simeq 7 \left[\frac{E_e}{50 \text{ TeV}}\right]^{-1} \text{ kpc}$$

Secondary photon energy

$$E_\gamma \simeq 8 \left[\frac{E_e}{50 \text{ TeV}}\right]^2 \text{ TeV}$$

Kalashev et al, 2007.14331

Conditions to detect 10 pG IGMF

Probe of the strongest fields $B \lesssim 10^{-11}$ G requires

(a) large primary point-source power in the 100 TeV energy range,

(b) detectability of extended emission in multi-TeV energy range, and

(c) presence of primordial IGMF in the several Mpc region around the source.

Kalashev et al, 2007.14331

Spectrum Mkn 421 and Mkn 501

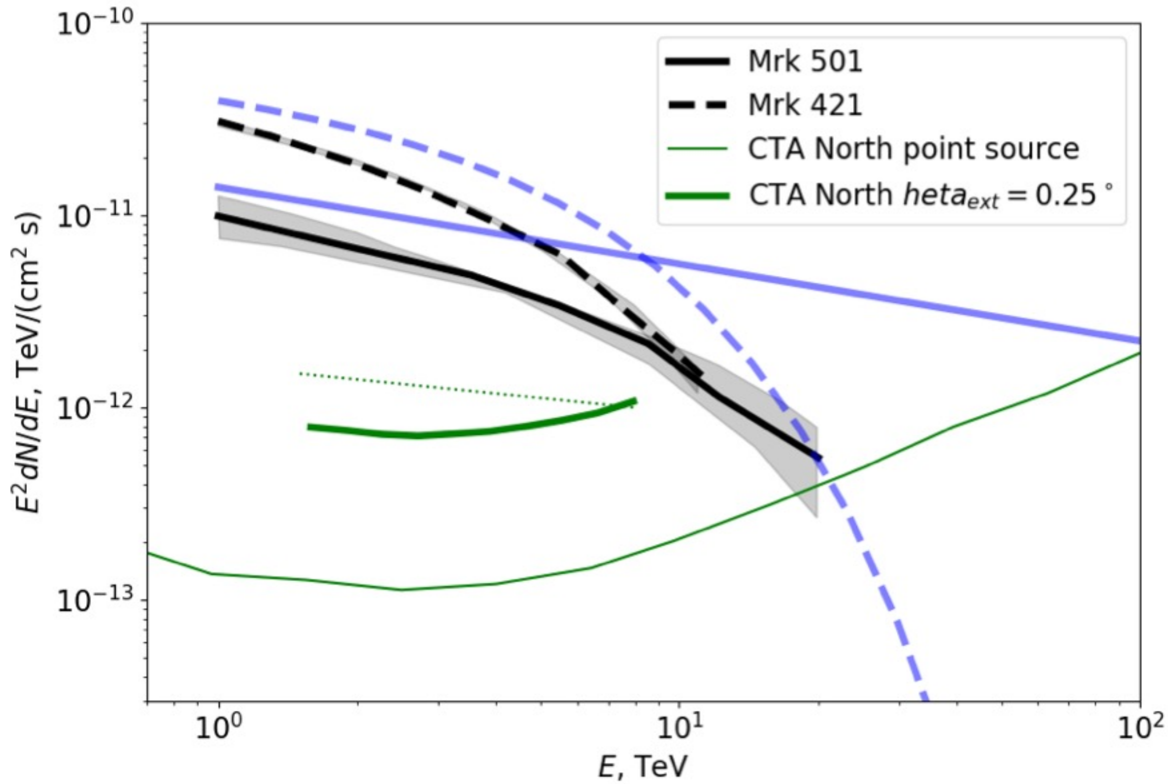

Kalashev et al, 2007.14331

IGMF on LOS to Mkn 501

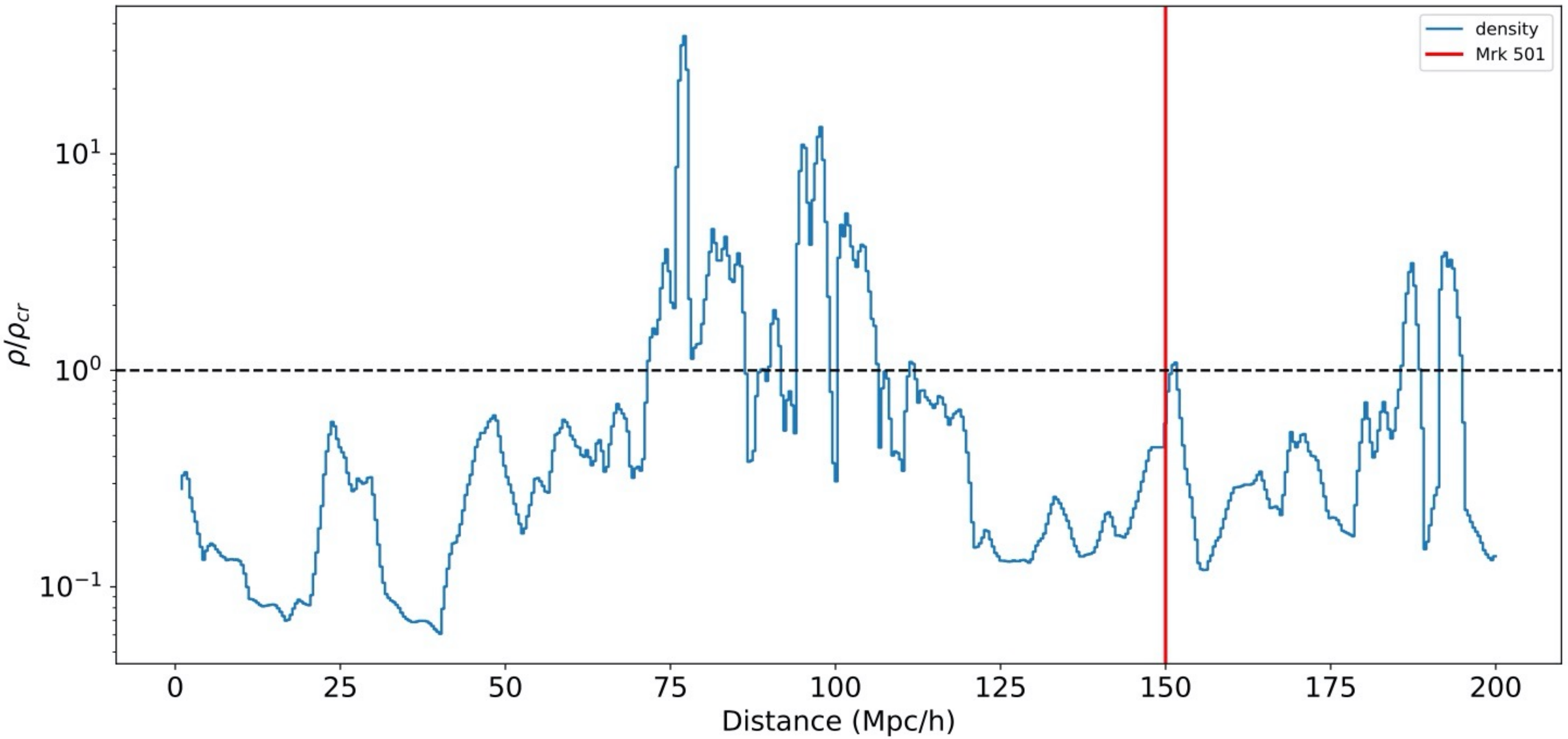

Kalashev et al, 2007.14331

Detection of extended emission around Mkn 501 by CTA North for 1-10 pG IGMF

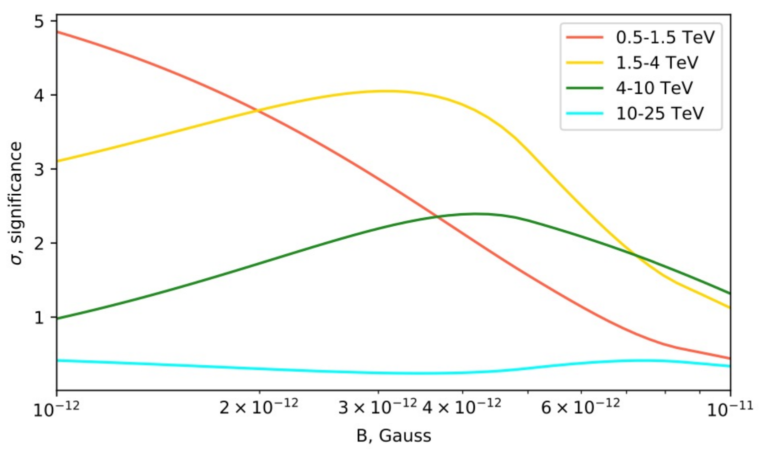

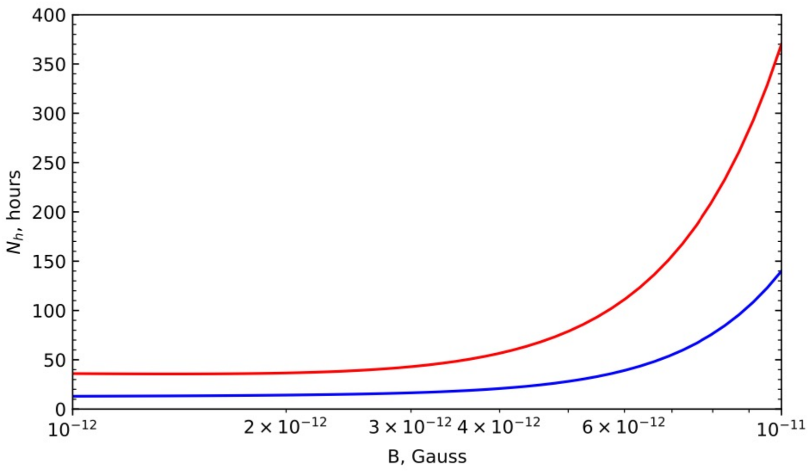

Kalashev et al, 2007.14331

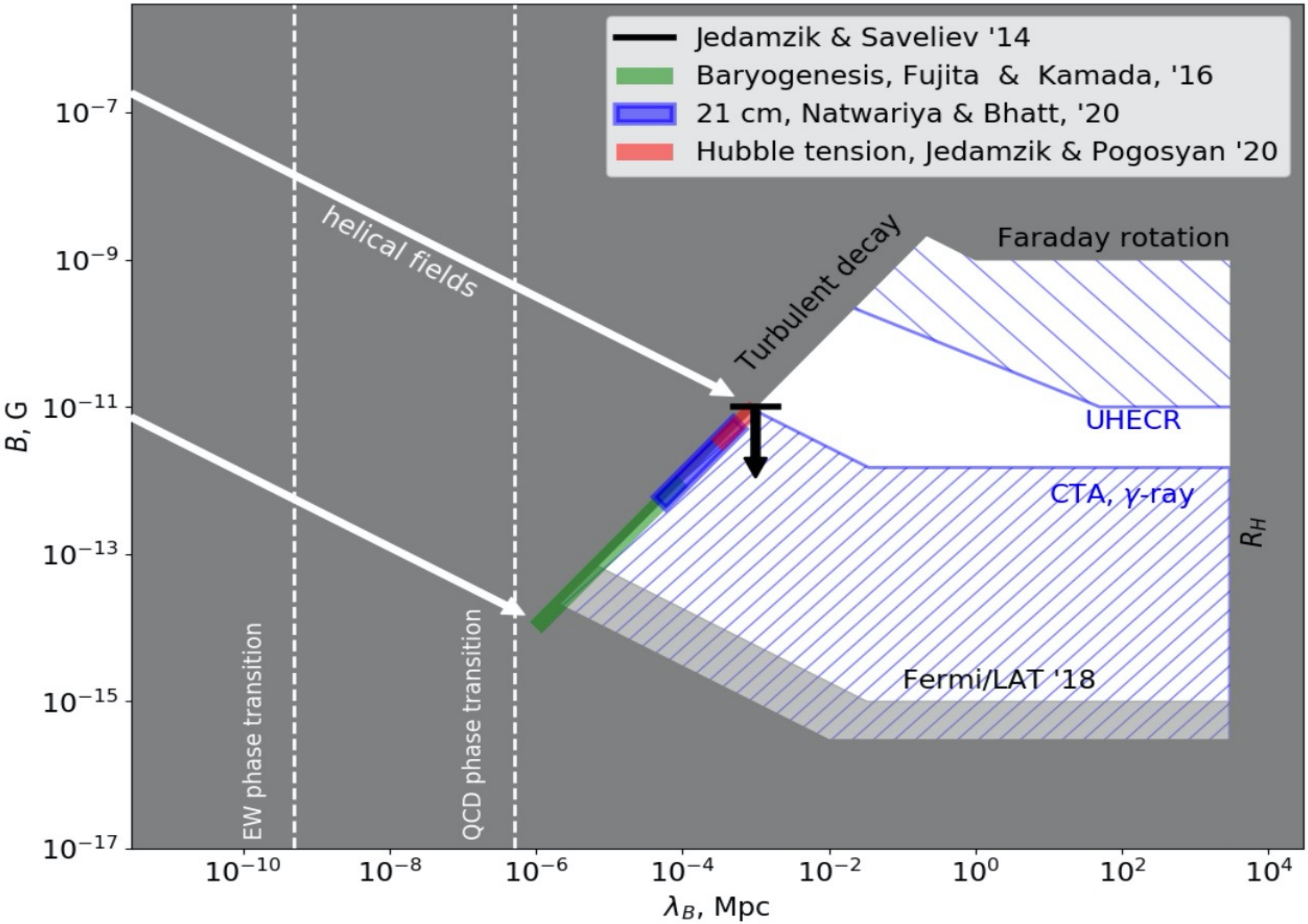

Kalashev et al, 2007.14331

Detection of Inter-Galactic Magnetic Field from inflation

BORG LSS and RAMSES MHD

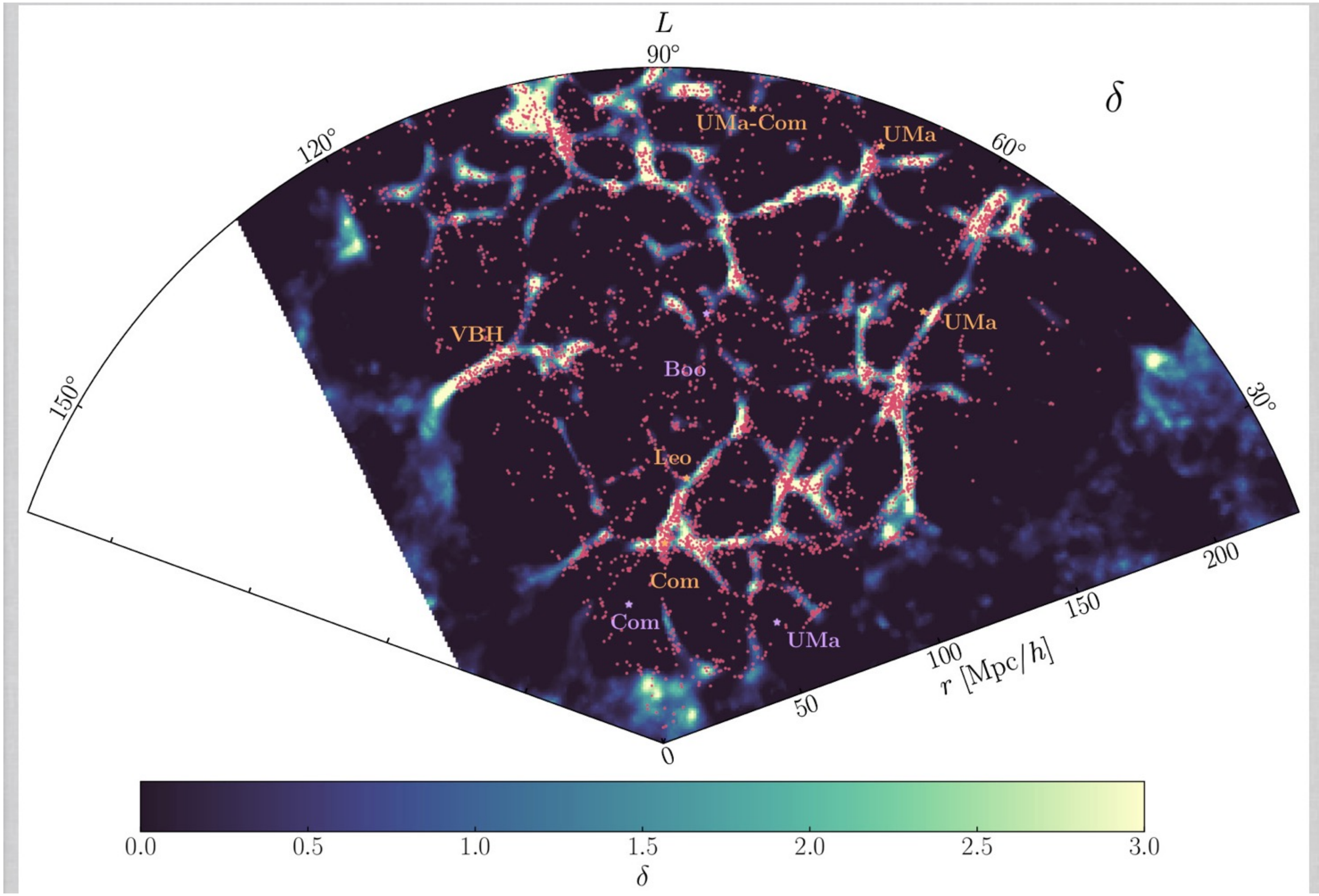

TeV blazars within 250 Mpc

Name	RA	Dec	z	$F_{1\mathrm{TeV}}$, TeV cm^{-2} s^{-1}
Mkn 421	166.11	38.21	0.031	2×10^{-11}
Mkn 501	253.47	39.76	0.033	1×10^{-11}
QSO B2344+514	356.77	51.7	0.044	4×10^{-12}
Mkn 180	174.11	70.16	0.046	8×10^{-13}
1ES 1959+650	299.99	65.15	0.047	6×10^{-12}
AP Librae	229.42	-24.37	0.04903	4×10^{-13}
TXS 0210+515	33.57	51.75	0.04913	2×10^{-13}

A.Korochkin et al, 2111.10311.

IGMF from inflation

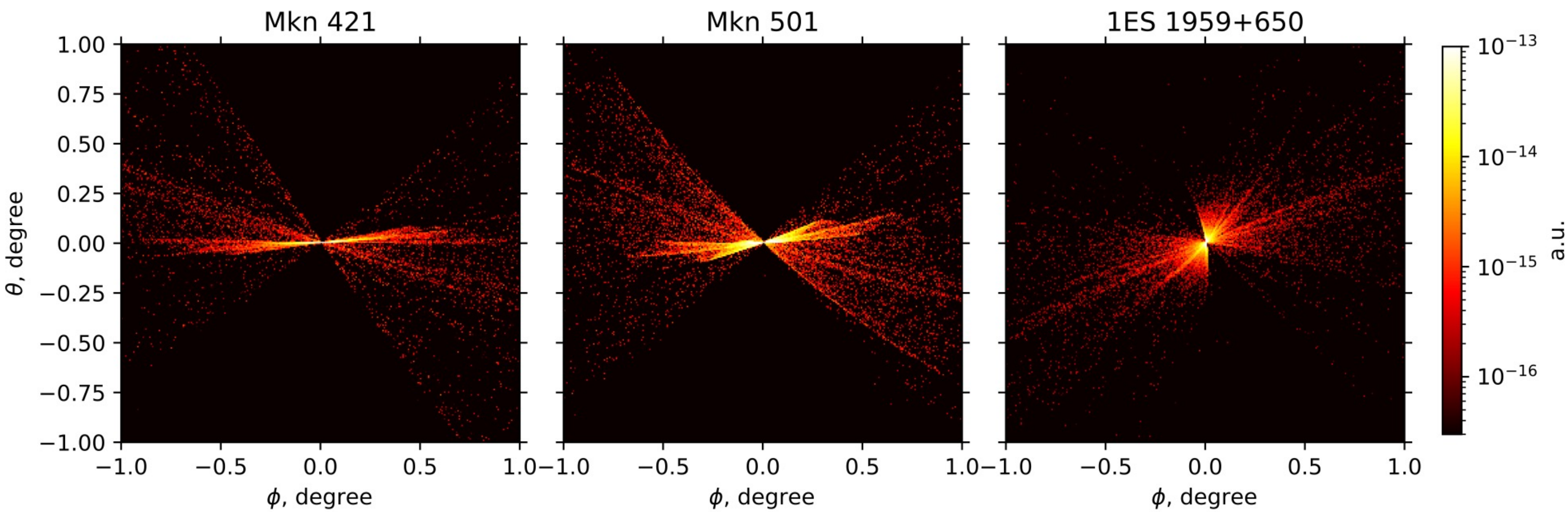

FIG. 4: Images of the extended emission signal in the energy range 200 GeV - 2 TeV for the three brightest sources in our sample. The assumed initial cosmological magnetic field strength is $B = 10^{-13}$ G. The direction of the jet axis coincides with the direction from the source to the observer and the jet opening angle is 5°.

A.Korochkin et al, 2111.10311.

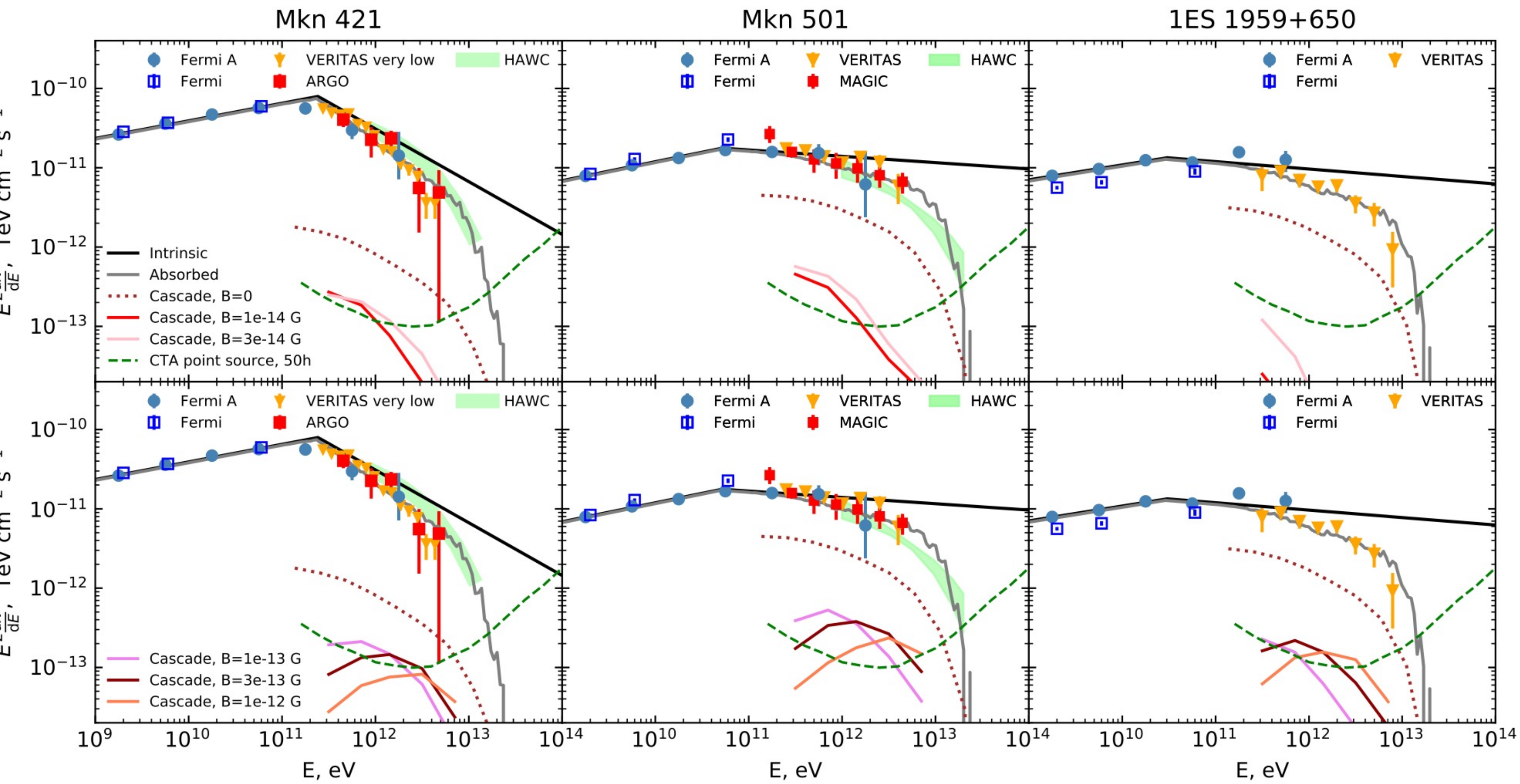

A.Korochkin et al, 2111.10311.

Inter-Galactic Magnetic Field detection with UHECR

TA sky map of Perseus-Pisces SC

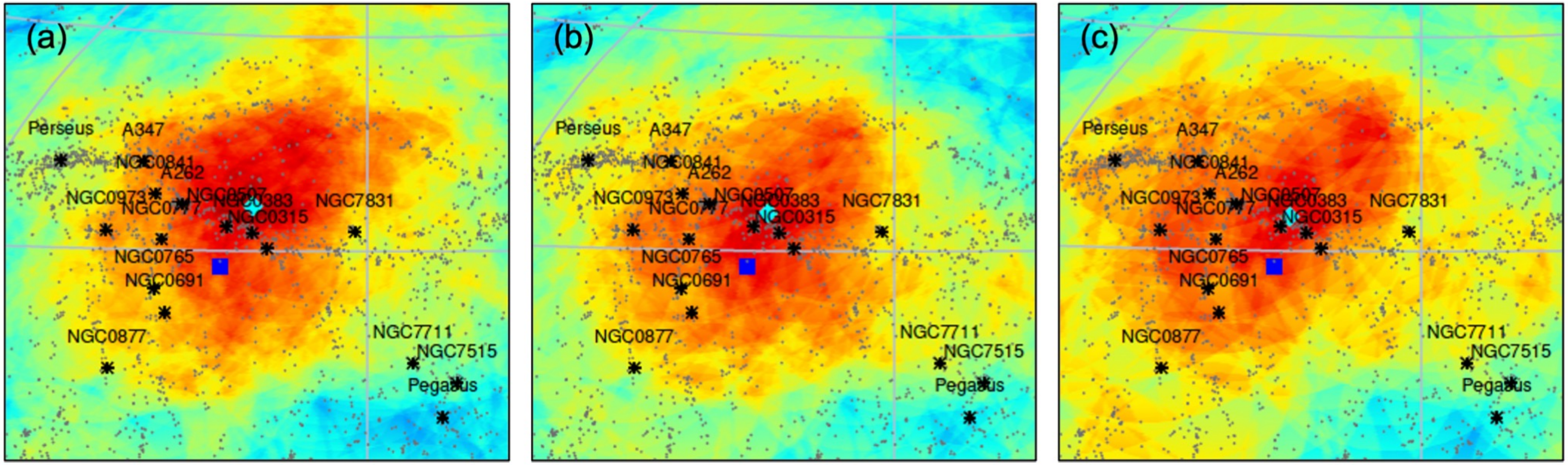

TA collaboration, 2110.14827

Deflection of UHECR C, He and p with 25 EeV energy by JF12 GMF

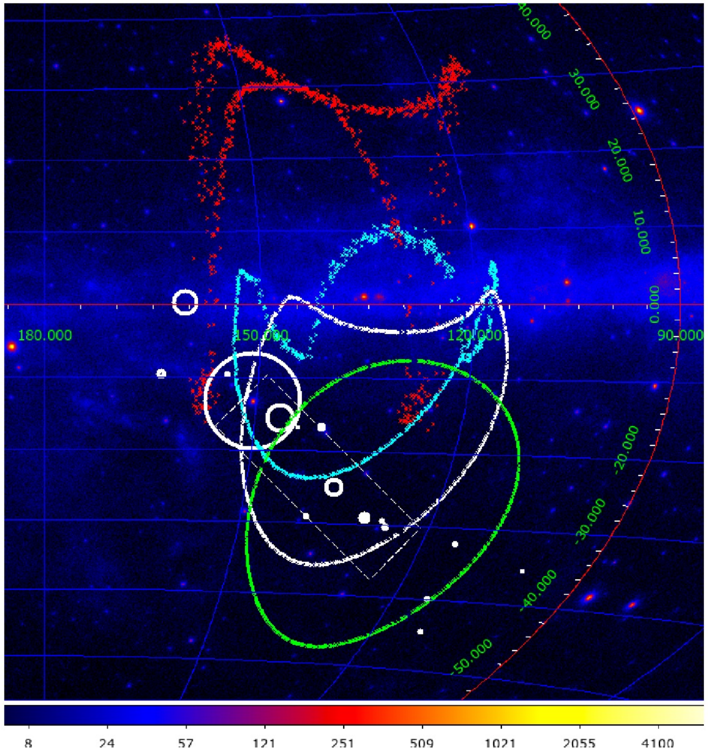

A.Neronov, D.S. and O.Kalashev, 2112.08202

Primordial IGMF and MF from astrophysical processes

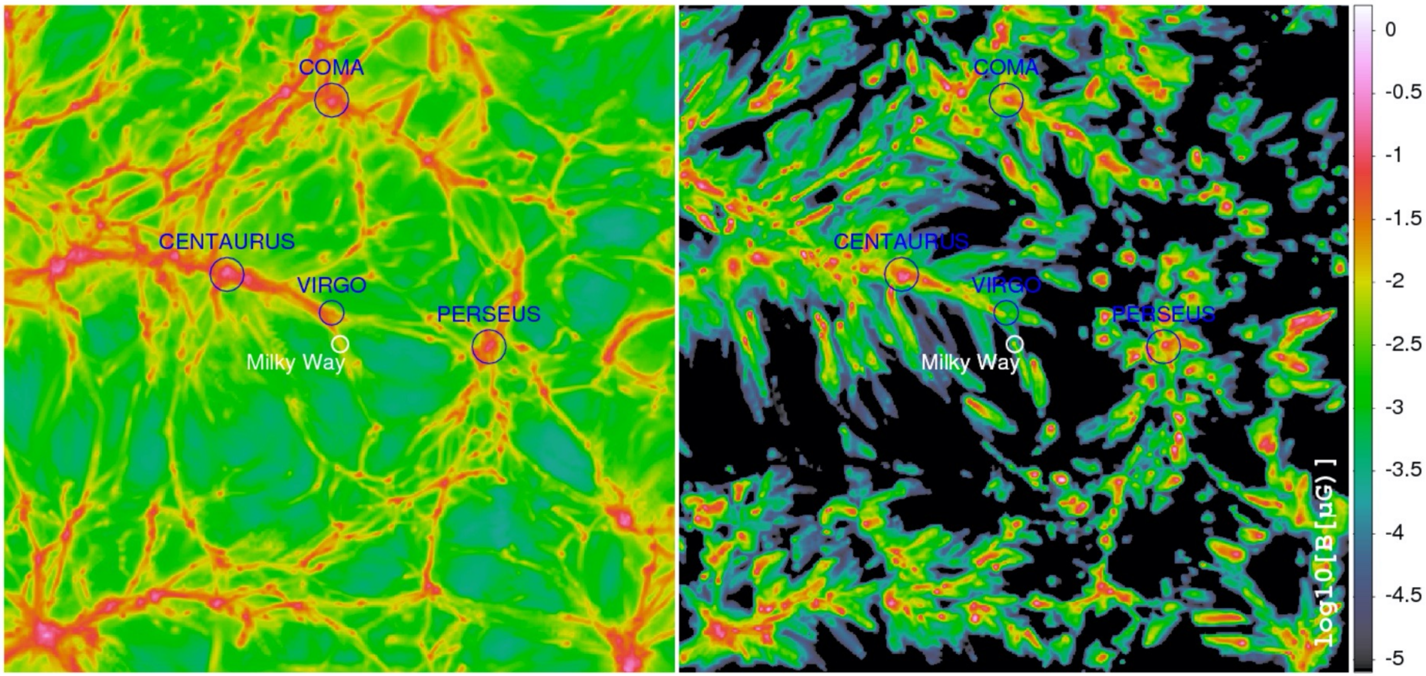

S. Hackstein et al, **MNRAS (2017) 1-11**, [1710.01353].

Limit on IGMF in Taurus void from UHECR observations

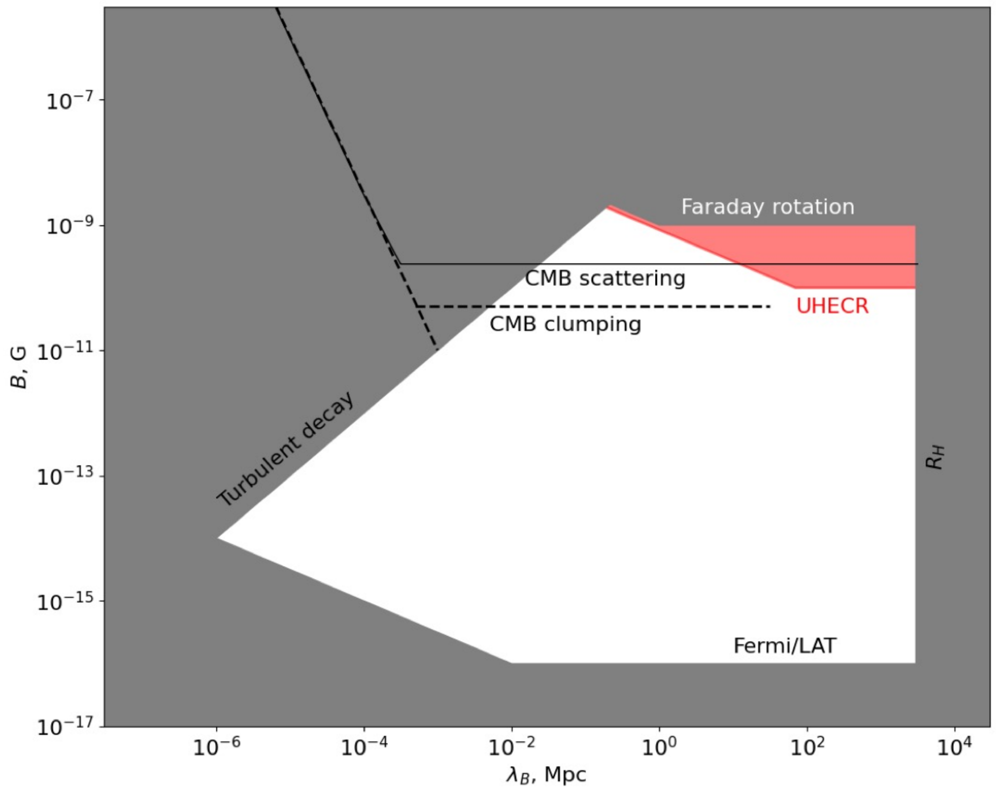

A.Neronov, D.S. and O.Kalashev, 2112.08202

Summary

- *Primordial magnetic field can be produced at inflation or in phase transitions in Early Universe. Magnetic field in 1-10 pG range help to solve H0 problem*
- *Pulsar timing arrays see common red noise consistent with GW signal. This signal can come from GW produced by primordial magnetic field at QCD phase transition. Shape potentially can be distinguished from BH pairs.*

Summary

- *Inter-Galactic Magnetic Fields in the voids of LSS with strength up to 10 pG can be found from high precision blazar spectra/time delay/ extended emission measurements by CTA*
- *Primordial MF from inflation can be found by measurement of extended emission with network of blazars*
- *IGMF in voids can be measured by UHECR detection from sources, Perseus-Pisces supercluster is first example*